PROBABILISTIC ASSESSMENT OF SUPPORT SCAFFOLD SYSTEMS

T. CHANDRANGSU, K.J.R. RASMUSSEN, & H. ZHANG

RESEARCH REPORT R911
JUNE 2010

ISSN 1833-2781

SCHOOL OF CIVIL ENGINEERING

THE UNIVERSITY OF SYDNEY

THE UNIVERSITY OF SYDNEY

SCHOOL OF CIVIL ENGINEERING

PROBABILISTIC ASSESSMENT OF SUPPORT SCAFFOLD SYSTEMS

RESEARCH REPORT R911

CHANDRANGSU, T., RASMUSSEN, K.J.R., AND ZHANG, H.

JUNE 2010

ISSN 1833-2781

ISSN 1833-2781

Published by:
School of Civil Engineering
The University of Sydney
Sydney NSW 2006
Australia

This report and other Research Reports published by the School of Civil Engineering are available at http://sydney.edu.au/civil

ABSTRACT

This research report presents comprehensive studies of the effects of uncertainties in material properties, initial geometric imperfections and joint stiffness on the ultimate system strength of multi-storey steel support scaffold systems through a rational statistical framework and a second-order inelastic finite element (advanced) analysis. A total of 36 stick-type steel scaffold systems with Cuplok joints in various configurations (different combinations of jack extensions, number of bays, and lift heights) are considered in the studies. The report also presents a reliability analysis of support scaffold systems to determine system resistance factors that can be used for the design by advanced analysis according to the LRFD statistical framework. The proposed system resistance factors based on the system target reliability index of 3.5 vary from 0.56 to 0.70, depending on the lift height and jack extensions.

KEYWORDS

Probabilistic study, Reliability analysis, System strength, Advanced analysis, Scaffold systems

TABLE OF CONTENTS

1 INTRODUCTION

Recently, researchers have studied the system strength predictions of steel frames by advanced analysis, involving uncertainties in loads and material yield strength (Buonopane and Schafer 2006). By nonlinear structural simulations and reliability analysis, system resistance factors based on certain target reliability for the design of steel frames by advanced analysis can be determined. The same concept is applied in this research. The strength of support scaffold systems is affected by variations in geometric and material parameters, particularly geometric imperfections, joint stiffness, loading eccentricity, and material yield stress. Thus, this report presents studies of the effects of these uncertainties on the ultimate strength of multi-storey steel support scaffold systems through a rational statistical framework and a second-order inelastic finite element (advanced) analysis. The report also presents a reliability analysis of support scaffold systems to determine system resistance factors that can be used in the design by advanced analysis according to the LRFD framework.

A total of 36 stick-type steel scaffold systems with Cuplok joints in various configurations (different combinations of jack extensions, number of bays, and lift heights) are considered in the following studies. The statistical data for the main inherent uncertainties has been acquired through actual field measurements (Chandrangsu and Rasmussen 2009a) and experimental tests (Chandrangsu and Rasmussen 2008). The nonlinear finite element models are created in Strand7 (Strand7 2009) based on the modelling concepts developed in Chandrangsu and Rasmussen (2009b). A Strand7 API subroutine is written in C++ to generate random inputs (geometric imperfections, joint stiffness, loading eccentricity, yield stress and section properties) for the finite element models, and then around 3,000 executions of advanced analyses for each of the 36 models (more than 100,000 advanced analyses in total) are used to predict variations in the ultimate system strength based on those parametric uncertainties. The mentioned procedures are also known as Monte Carlo simulations. The inherent uncertainties and the model uncertainty are propagated through Monte Carlo simulations to obtain the statistics of system strength. By comparison with full-scale load tests (CASE 2006), the bias and variability of advanced analysis are estimated. The first-order second-moment method (FOSM) and first-order reliability method (FORM) are then employed to estimate the reliability of support scaffold systems. Finally, system resistance factors are proposed for various system configurations to be used with the design of support scaffold systems by advanced analysis.

2 ANALYSIS MODELS FOR PROBABILISTIC ASSESSMENT

Thirty six configurations of steel support scaffold systems with Cuplok joints are chosen to be representative of those encountered in scaffold construction. The systems are categorised by number of bays (1x1 bay, 3x3 bays, 3x6 bays, and 9x9 bays), lift heights (1.0 m, 1.5 m, and 2.0 m), and jack extensions (100 mm, 300 mm, and 600 mm). The same bay width of 1829 mm (frequently used in construction) and 3 lifts (same number of lifts) are selected for all systems. Figures 1 to 4 show the system configurations used in the studies. The

standards, attached with Cuplok joints, are made from cold-formed circular steel tube (CHS) grade 450 MPa with nominal outside diameter of 48.3 mm and thickness of 4 mm. The grade 350 MPa (CHS) ledgers with end blades are of nominal outside diameter of 48.3 mm and thickness of 3.2 mm. The telescopic (CHS) braces with hook ends are made of 48.3 mm x 4.0 mm outer tube and 38.2 mm x 3.2 mm inner tube with nominal yield stress of 400 MPa. The adjustable jacks are made of 36 mm diameter threaded steel rod of grade 430 MPa. The jack extensions at the top and bottom of the frame are set to equal. The base plates are 180 mm x 180 mm x 10 mm in dimension with a nominal yield stress of 250 MPa. The spigot joints are assumed to be located at the mid-height of the second and third lifts. There are no spigots in the bottom lift based on general construction practice. All the systems are considered fully braced. For the case of 9x9 bays, the frame is braced every fourth bay according to general practice and no corner braces are used, as illustrated in Figure 4. Also, there are no corner braces for the cases of 3x3 bays and 3x6 bays, as shown in Figures 2 and 3, respectively.

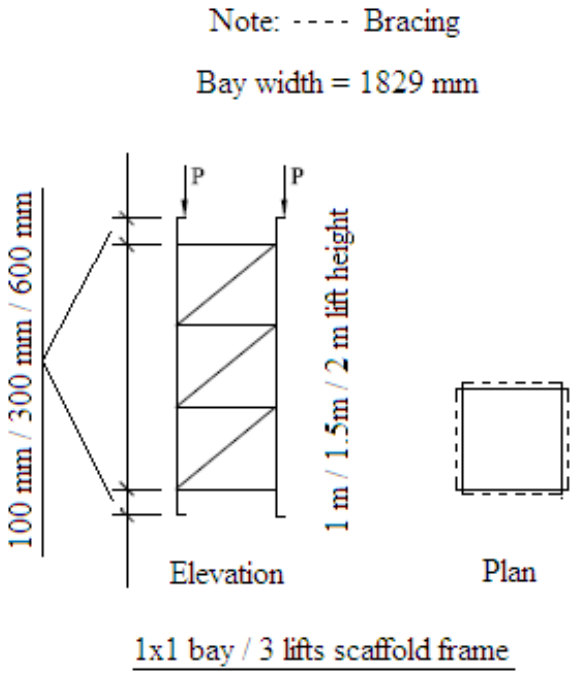

Figure 1: 1x1 bay scaffold configuration in the studies

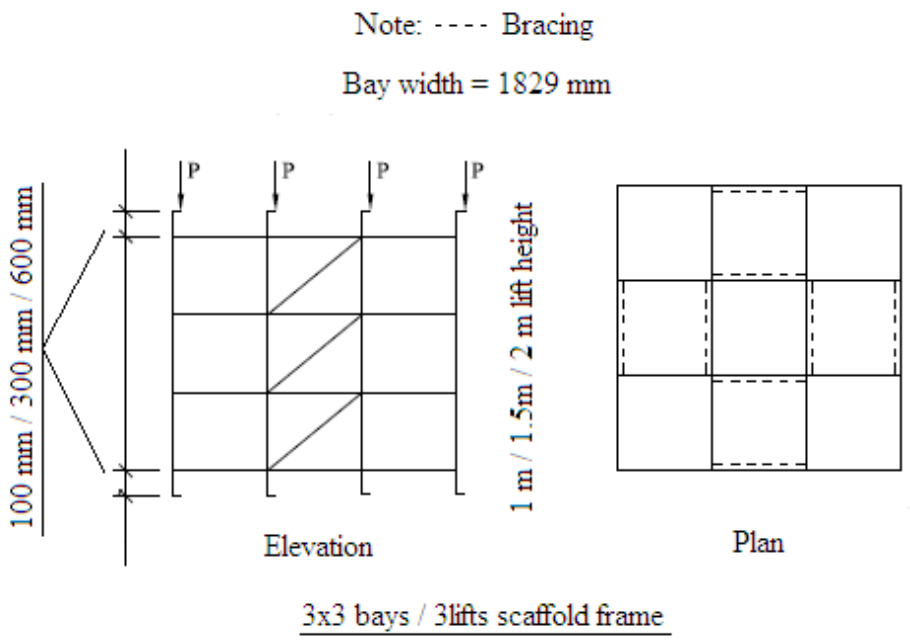

Figure 2: 3x3 bays scaffold configuration in the studies

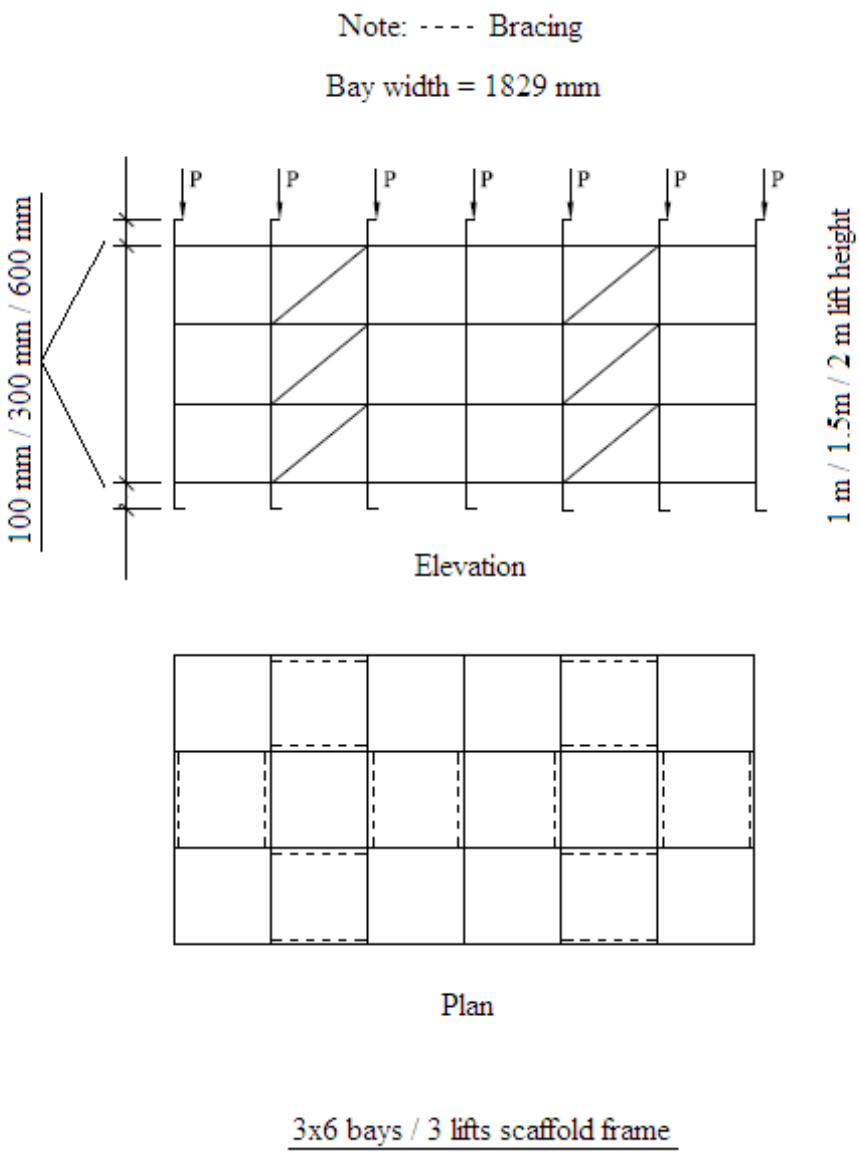

Figure 3: 3x6 bays scaffold configuration in the studies

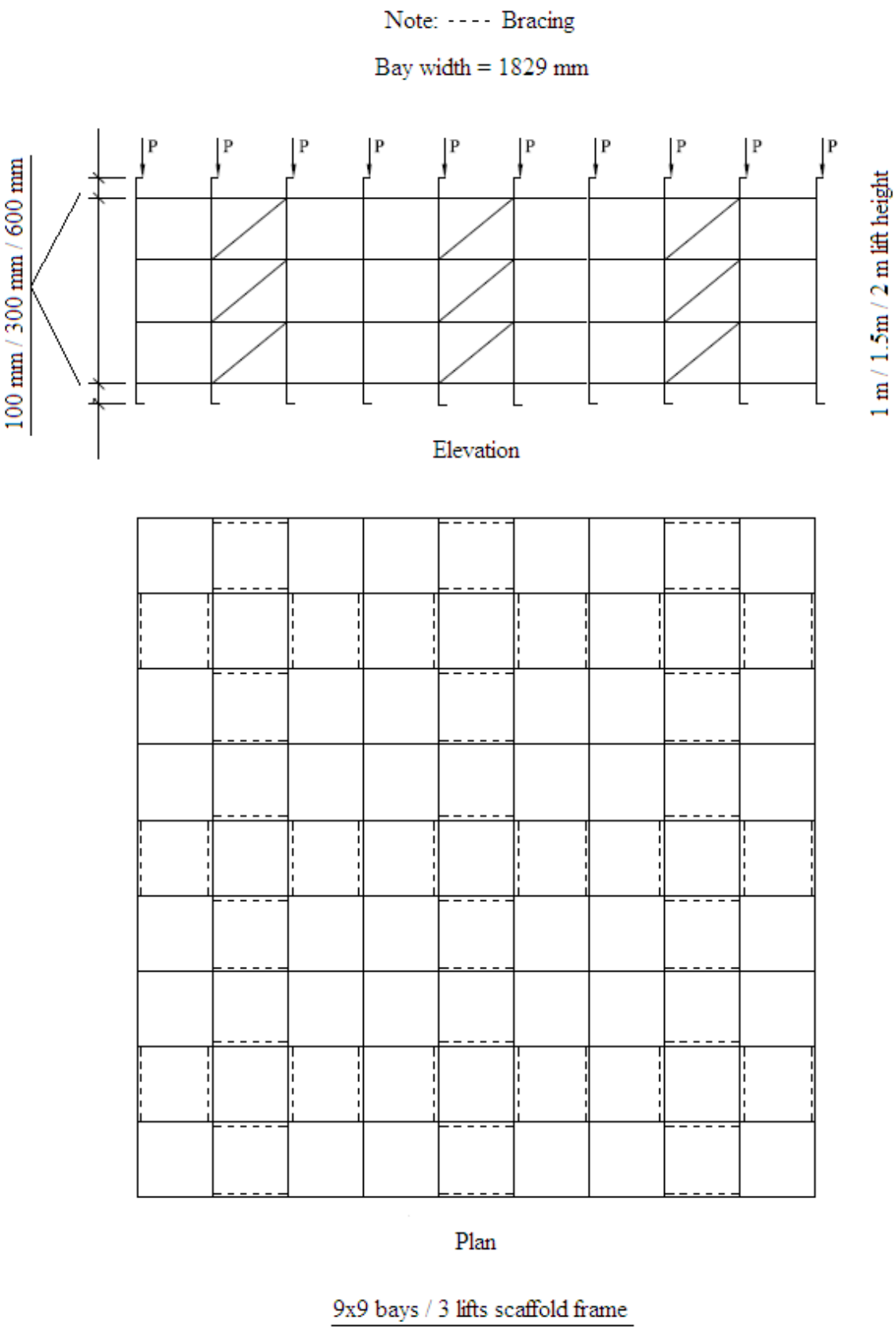

Figure 4: 9x9 bays scaffold configuration in the studies

The three-dimensional finite element models have been created with the same modelling concept presented in Chandrangsu and Rasmussen (2009b) for Monte Carlo simulations. The models consist of spigot joints, nonlinear moment-rotation joint stiffness for the standard-to-ledger connections, brace connections with 1.8 kN/mm axial spring stiffness and 60 mm offset from the nodal points, base plate eccentricity, loading eccentricity, geometric imperfections implemented directly at the nodes, and Ramberg-Osgood material model for all of the scaffold components. For the top boundary conditions, the rotational stiffness about the x-axis is assumed to be rigid, corresponding to the negligible strong axis bending of the supported timber bearer; however, the y-axis bending stiffness is taken as 40 kNm/rad as obtained from the model calibrations in Chandrangsu and Rasmussen (2009b). For the bottom boundary conditions, the base plate model is applied with the eccentricity of 15 mm (close to maximum allowable bottom eccentricity specified in AS 3610 by Standard Australia 1995) to each upright. Equal vertical point loads are applied with random variations in eccentricity on top of each U-head screw jack. All frames are assumed to be braced laterally at the top of the U-head screw jacks. Figure 5 shows a typical finite element model of the 3x6 bays, 3 lifts, and 1 m lift height with 100 mm jack extensions.

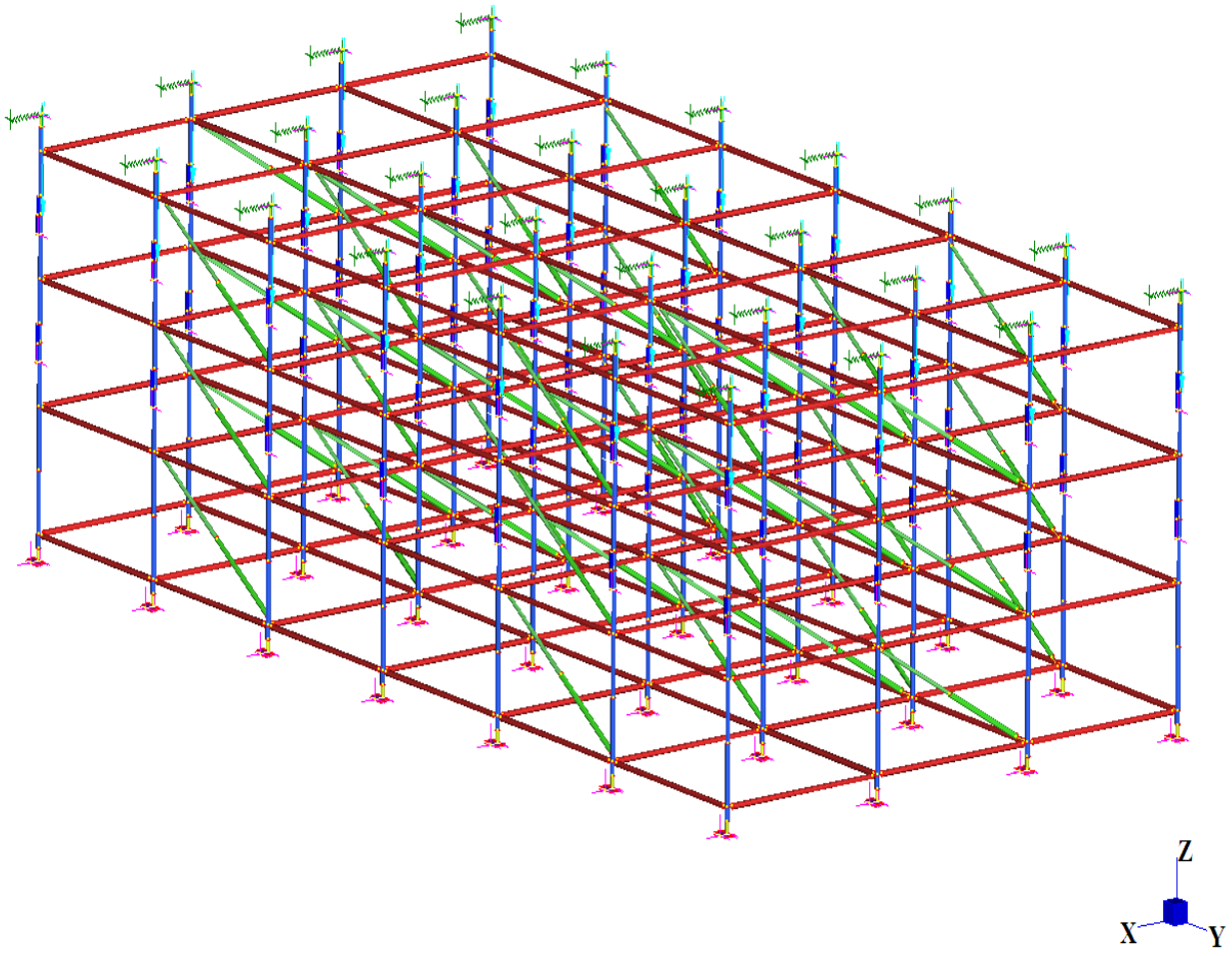

Figure 5: Typical finite element model for Monte Carlo simulations

3 UNCERTAINTIES IN SUPPORT SCAFFOLD SYSTEMS

In scaffold construction, components such as standards, ledgers, jacks, joints and base plates are reused from one job to another and new members are mixed with old ones. Most of the components come with imperfections, whether from repeated use or the manufacturing process. As a result, scaffold systems are prone to many uncertainties that can be characterised into variations in geometric and material properties, as well as joint stiffness. In this research, the uncertainties being considered include cross-sectional area and moment of inertia of the standards and jacks, yield stress of the standards and jacks, joint stiffness for standard-to-ledger connections, initial geometric imperfections, and loading eccentricity. These uncertainties are treated as random variables in the Monte Carlo simulations to obtain the statistics of the system strength.

3.1 CROSS-SECTIONAL AREA AND MOMENT OF INERTIA

Due to uncertainty in manufacturing environments, scaffold components can possess different dimensions that lead to variations in the cross-sectional area and moment of inertia of the sections. This research considers cross-sectional area and moment of inertia of the main loaded components, which are the standards and jacks, as random variables, while those of other components are assumed deterministic at their mean values (taken conservatively to be the same as their nominal values in the absence of available data). For the purpose of Monte Carlo simulations, the statistical data for the cross-sectional area and moment of inertia of the standards and jacks is obtained from dimensional measurements of around 80 second-hand standards and jacks. The mean cross-sectional areas of the standards and jacks are computed to be 556.69 mm^2 and 1017.876 mm^2, respectively, with a coefficient of variation (COV) of 0.05 for both. The mean moments of inertia of the standards and jacks are 137675.8 mm^4 and 82447.96 mm^4, respectively, with a coefficient of variation (COV) of 0.05 for both. Both cross-sectional area and moment of inertia of the standards and jacks are statistically modelled as lognormal distributions. For each simulation, one element in the model possesses its own random values of cross-sectional area and moment of inertia.

3.2 YIELD STRESS

Because of uncertainty in manufacturing process, each type of scaffold components can show a significant variation in yield stress which affects the strength of scaffold systems. For the purpose of Monte Carlo simulations, the statistical data for the (static) yield stress is obtained from the literature (Galambos and Ravindra 1978). The mean yield stress is assumed to be $1.10F_y$ with a coefficient of variation (COV) of 0.1, where F_y represents the minimum specified (nominal) yield stress for the grade of steel. Only the yield stresses of the main components in loading (the standards and jacks) are important and considered as random variables in the simulations, whereas those of other components are assumed deterministic at their mean values (Chandrangsu and Rasmussen 2009b). Therefore, the mean yield stresses of the standards and jacks are 495 MPa and 473 MPa, respectively with a coefficient of variation (COV) of 0.1 for both. They are

statistically modelled as normal distributions in the simulations. In one simulation, each element in the model has its own random value of yield stress.

3.3 JOINT STIFFNESS

The joints between standard and ledger present uncertain behaviours due to imperfections from repeated use and consequent varying degrees of fixity. In order to predict the overall stability of the frame and strength of the system, the standard-to-ledger connections must be modelled correctly. Cuplok joints are considered in this research as standard-to-ledger connections for support scaffold systems. Experimental joint tests (Chandrangsu and Rasmussen 2008) have shown that Cuplok joints behave as semi-rigid connections and usually show looseness with small stiffness at the beginning of loading due to a lack of fit (Figure 6(a)). For Monte Carlo simulations, a tri-linear joint model (Chandrangsu and Rasmussen 2008) as shown in Figure 6(b) is used to approximate the relation between the moment and rotation of Cuplok joints.

Since probabilistic assessment of the strength of scaffold systems depends mainly on the stiffness of joint bent in the vertical plane, but not in the horizontal plane, only variation in the vertical bending stiffness is considered, and the modelling of the horizontal bending stiffness can be assumed to be deterministic using the mean values for the tri-linear curve, as presented in Tables 1-2 for bending about the vertical axis. For practicality in probabilistic modelling, the values of β_1, β_2 and β_3 are assumed to be deterministic, taken as their mean values; however, the variations of k_1, k_2, and k_3 for bending about the horizontal axis are taken into account. The coefficients of variation of the joint stiffness for k_1, k_2, and k_3 for bending about the horizontal axis (vertical bending stiffness) for different joint configurations are presented in Table 3. Each joint stiffness is statistically modelled as a normal distribution in the simulations as explained in Chandrangsu and Rasmussen (2008).

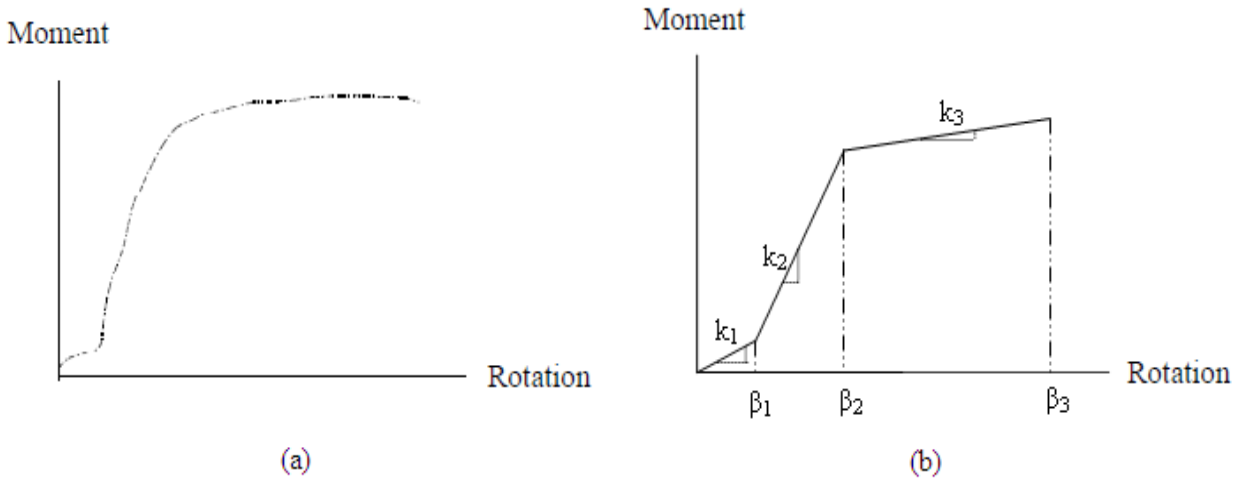

Figure 6: Graph of (a) typical Cuplok joint behaviour (b) tri-linear joint model

Table 1: Mean Cuplok joint stiffness (kNm/rad)

	Bending stiffness about horizontal axis (kNm/rad)			Bending stiffness about vertical axis (kNm/rad)		
Joint configuration	k_1	k_2	k_3	k_1	k_2	k_3
4-way	39	102	5.3	15	7.5	0.8
3-way	36	87	5.1	14	7	1
2-way	41	77	4.6	7.5	5	1.5

Table 2: Mean rotation for Cuplok joints (rad)

	Rotation about horizontal axis (rad)			Rotation about vertical axis (rad)		
Joint configuration	β_1	β_2	β_3	β_1	β_2	β_3
4-way	0.014	0.036	0.16	0.02	0.04	0.1
3-way	0.012	0.036	0.16	0.02	0.04	0.1
2-way	0.007	0.036	0.16	0.02	0.04	0.1

Table 3: Coefficient of variation of Cuplok joint stiffness

	Bending about horizontal axis		
Joint configuration	k_1	k_2	k_3
4-way	0.22	0.18	0.30
3-way	0.38	0.21	0.37
2-way	0.35	0.20	0.46

3.4 INITIAL GEOMETRIC IMPERFECTIONS

Scaffold systems are slender in nature, thus the strength and behaviour of support scaffolds are susceptible to adverse 2^{nd} order member P-δ and frame P-Δ effects. Therefore, initial geometric imperfections producing 2^{nd} order effects must be considered in the analysis models. Two types of initial geometric imperfections, specifically imperfections from storey out-of-plumb (initial frame sway) and out-of-straightness of the standards (initial member crookedness) are considered in the Monte Carlo simulations. It is obvious that there is a lack of data available for the out-of-straightness and out-of-plumb of scaffold systems in the literature. The Australian standard (Standard Australia 1998) allows a maximum out-of-straightness of $L_h/1000$ and a maximum out-of plumb of H/400, where L_h is the column length and H is the storey height. Nevertheless, these allowable values are proposed for steel buildings rather than scaffold systems. In addition, the out-of-straightness of the standards often exceeds the tolerance values imposed by the codes, especially where the standards are connected with spigot joints, as shown in the survey data in (Chandrangsu and Rasmussen 2009a).

The observed imperfection data shows that the initial out-of-straightness of standards without spigots has a mean of $L_h/2500$ and a COV of 0.75. However, the initial out-of-straightness of standards with spigot joints increases considerably at the location of the spigot joint as presented in Chandrangsu and Rasmussen (2009a) to have a mean of $L_h/770$ and a COV of 0.615. The probability distribution for the member out-of-straightness is taken as lognormal (Chandrangsu and Rasmussen 2009a). The storey out-of-plumb is fitted to a normal distribution with a mean of H/625 and a COV of 0.313 (Chandrangsu and Rasmussen 2009a). Out-of-straightness values of the standards and the storey out-of plumb are applied to the analysis models, treating each standard independently (uncorrelated) and assigning random magnitude and direction of out-of-straightness in the x-axis for each standard, as shown in Figure 5. Table 4 shows the statistical data for the initial geometric imperfections used in the simulations.

Table 4: Statistical data for initial geometric imperfections used in the simulations

Random variable	Mean	COV	Distribution
Out-of-straightness of the standards without spigot joints	$L_h/2500$	0.75	Lognormal
Out-of-straightness of the standards with spigot joints	$L_h/770$	0.615	Lognormal
Storey out-of-plumb	H/625	0.313	Normal

3.5 LOADING ECCENTRICITY

The strength of support scaffold systems is highly influenced by the loading eccentricity between the timber bearer and the U-head. As a result, loading eccentricity must be included in the probabilistic assessment of the strength of support scaffold systems. The Australian standard for formwork (Standard Australia 1995) limits the eccentricity at 40 mm or 25% of the bearer width, whichever is less (18.75 mm for the Cuplok systems investigated herein).

It can be seen from the data obtained from on-site measurements of the loading eccentricity in Chandrangsu and Rasmussen (2009a) that the mean value (18.10 mm) is approximately equal to the limit imposed by the code; however, for the purpose of Monte Carlo simulations the loading eccentricity is limited at not more than 55 mm (maximum possible loading eccentricity for the studied system) with the mean of 18.10 mm and a COV of 0.608 in the analysis models. The loading eccentricity is modelled by a lognormal distribution in the simulations and applied to the analysis models as random in magnitude and direction in the x-axis, direction perpendicular to the timber bearers, as shown in Figure 5. Table 5 summarises the statistical data for the initial loading eccentricity used in the Monte Carlo simulations.

It should be noticed that eccentricity can also occur at the bottom due to uneven or sloped ground. The amount of base eccentricity depends largely on ground surface irregularities. The Australian standard AS 3610 (Standard Australia 1995) specifies an expected base eccentricity of no more than 40 mm or $b_p/4$, whichever is less, where b_p is the stiff portion of bearing of an end plate. For example, $b_p/4$ is 17 mm for the support scaffold system studied in this research which is less than 40 mm; therefore, the expected base eccentricity of the system is no more than 17 mm. Since there is no statistical data for the base eccentricity available in the literature and acquisition of such data is difficult and subjective, the bottom eccentricity is assumed conservatively to be 15 mm applied in the same direction to each upright with the base plate modelling concept presented in Chandrangsu and Rasmussen (2009b).

Table 5: Statistical data for loading eccentricity used in the simulations

Random variable	Mean	COV	Distribution
Loading eccentricity	18.10 mm	0.608	Lognormal

4 ULTIMATE STRENGTH OF SUPPORT SCAFFOLD SYSTEMS

Once the three-dimensional finite element models of 36 configurations of steel support scaffold systems with Cuplok joints had been created, each model was modified for each analysis with the generated values of random variables considered herein through an API subroutine, and around 3,000 advanced analyses on each model were performed in Strand7 (2009) to obtain the statistics of the ultimate strength for the 36 system configurations.

4.1 MONTE CARLO SIMULATION RESULTS

The relative frequency histograms of the ultimate strength of the 36 different system configurations are presented in Figures 7-42. The mean ($\overline{R}$) and coefficient of variation (V_R) for the system ultimate strength of the 36 systems studied are summarised in Table 6.

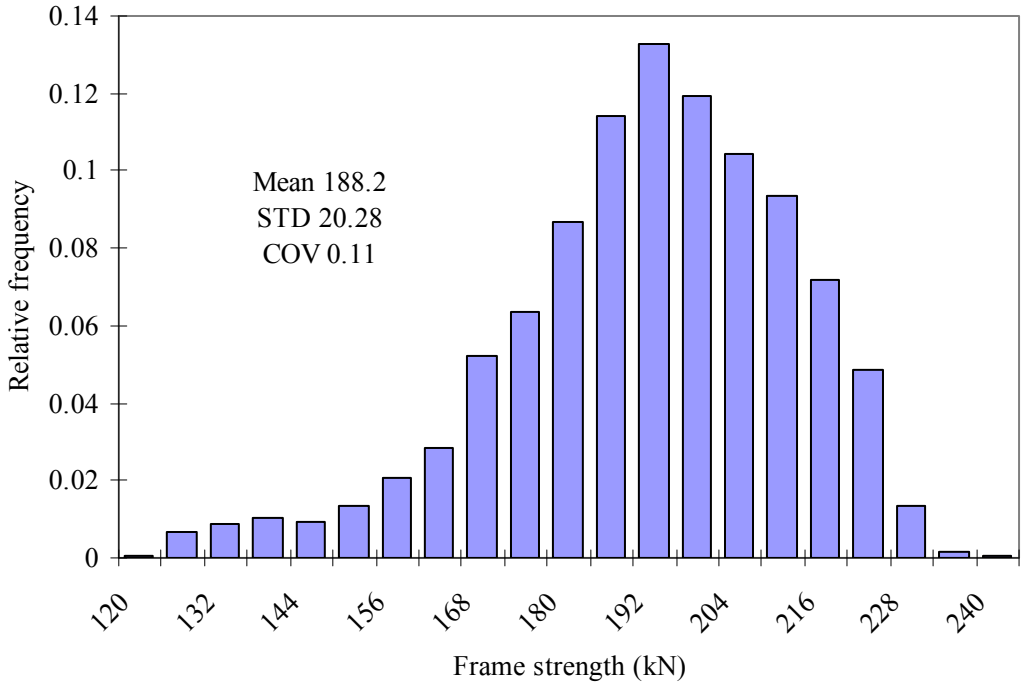

Figure 7: Histogram for the ultimate strength of 1x1 bay, 1 m lift height, 3 lifts, and 100 mm top and bottom jack extensions support scaffold frame

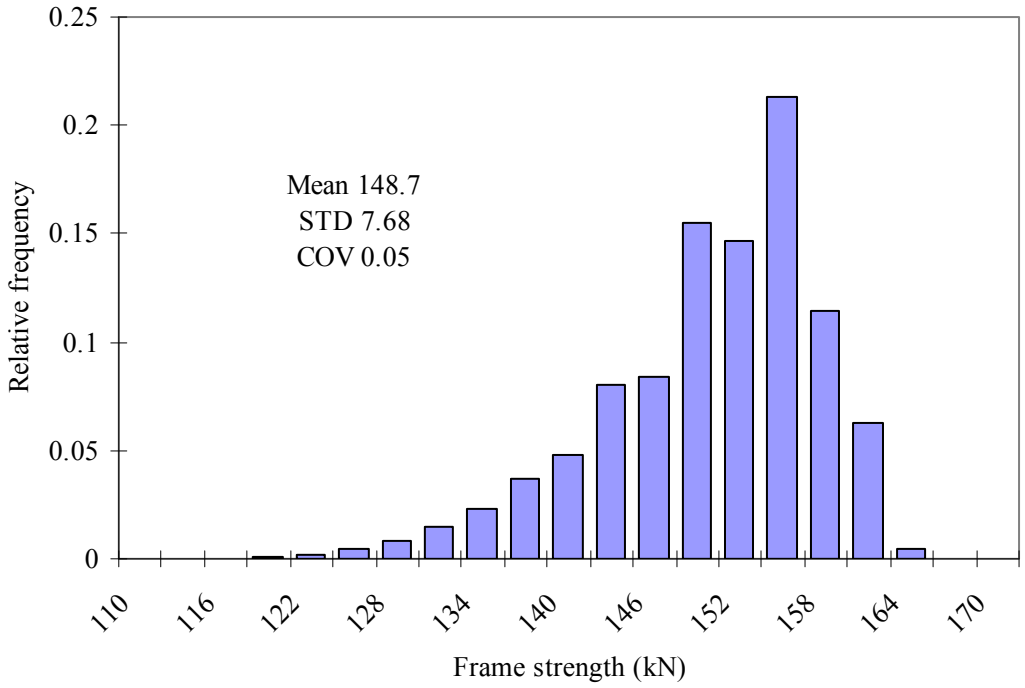

Figure 8: Histogram for the ultimate strength of 1x1 bay, 1 m lift height, 3 lifts, and 300 mm top and bottom jack extensions support scaffold frame

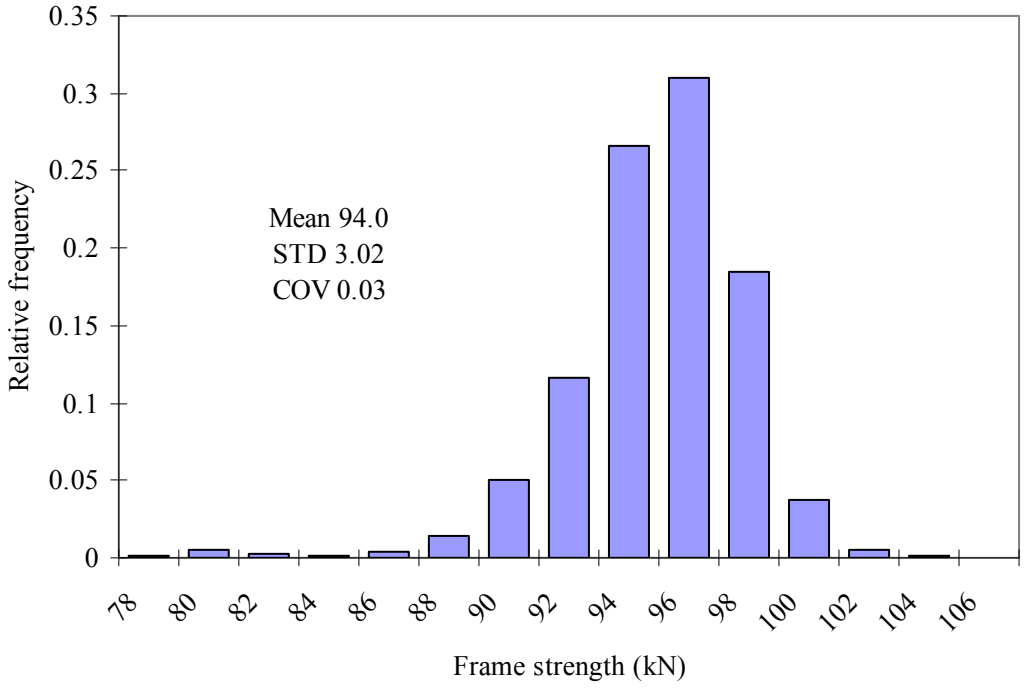

Figure 9: Histogram for the ultimate strength of 1x1 bay, 1 m lift height, 3 lifts, and 600 mm top and bottom jack extensions support scaffold frame

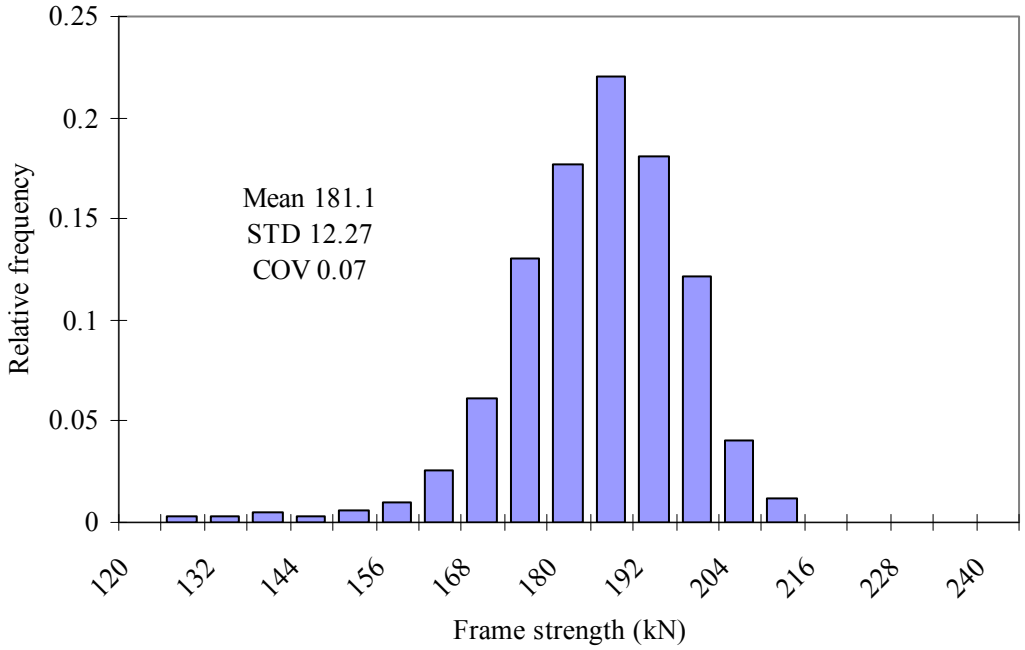

Figure 10: Histogram for the ultimate strength of 3x3 bays, 1 m lift height, 3 lifts, and 100 mm top and bottom jack extensions support scaffold frame

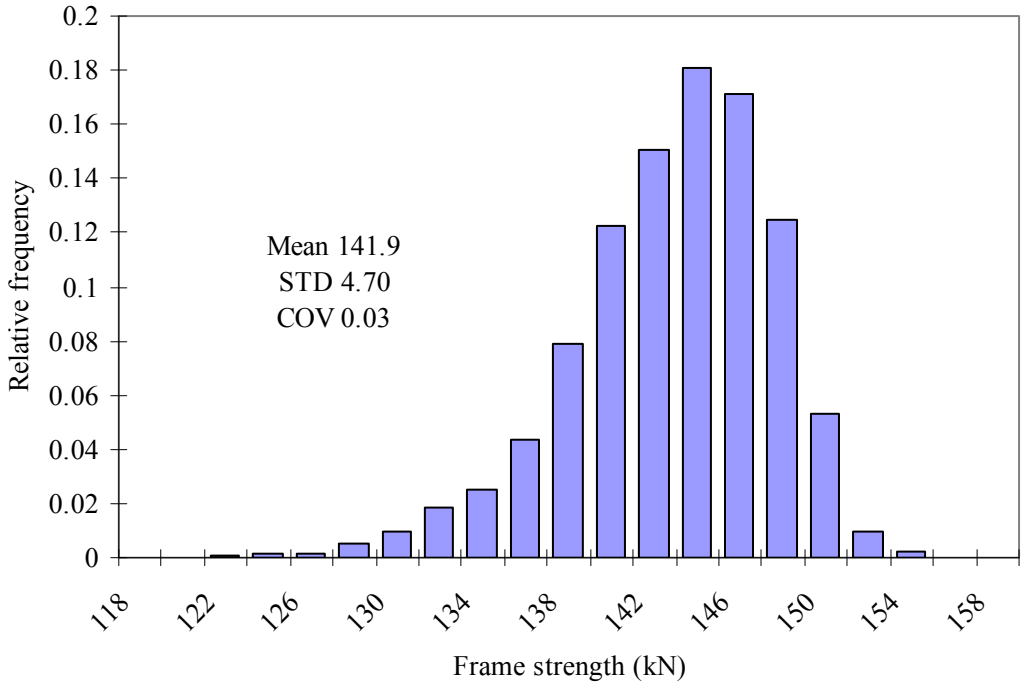

Figure 11: Histogram for the ultimate strength of 3x3 bays, 1 m lift height, 3 lifts, and 300 mm top and bottom jack extensions support scaffold frame

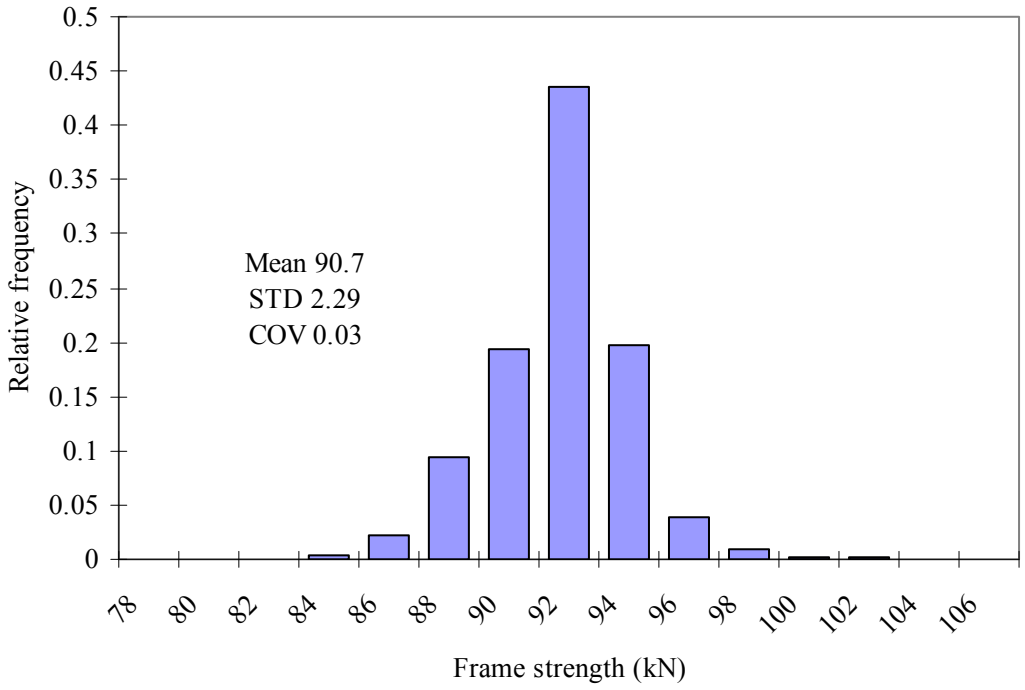

Figure 12: Histogram for the ultimate strength of 3x3 bays, 1 m lift height, 3 lifts, and 600 mm top and bottom jack extensions support scaffold frame

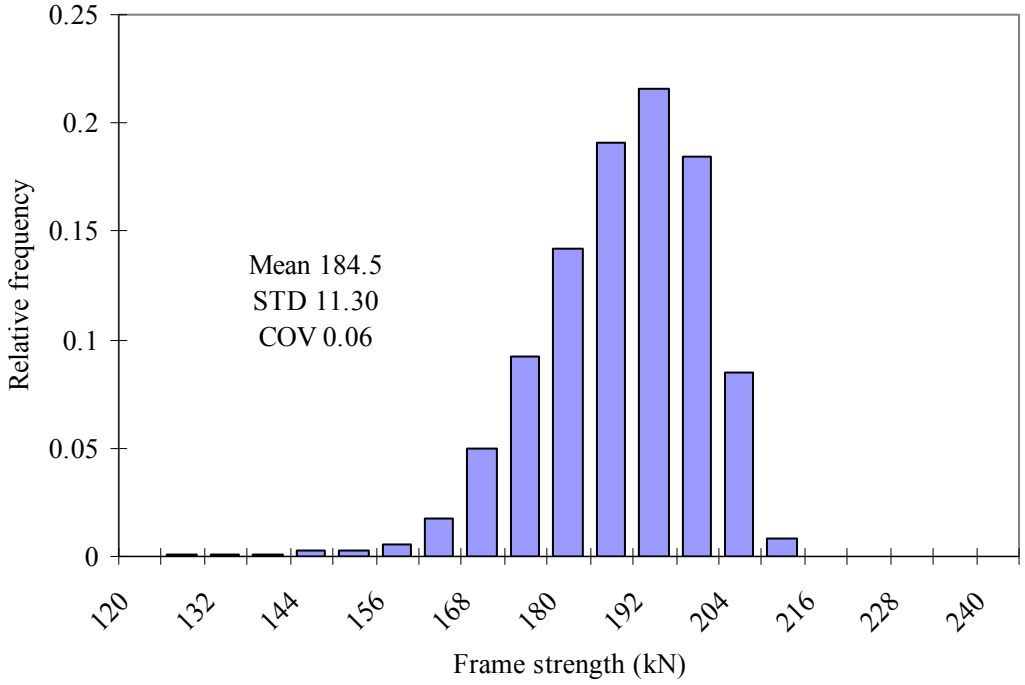

Figure 13: Histogram for the ultimate strength of 3x6 bays, 1 m lift height, 3 lifts, and 100 mm top and bottom jack extensions support scaffold frame

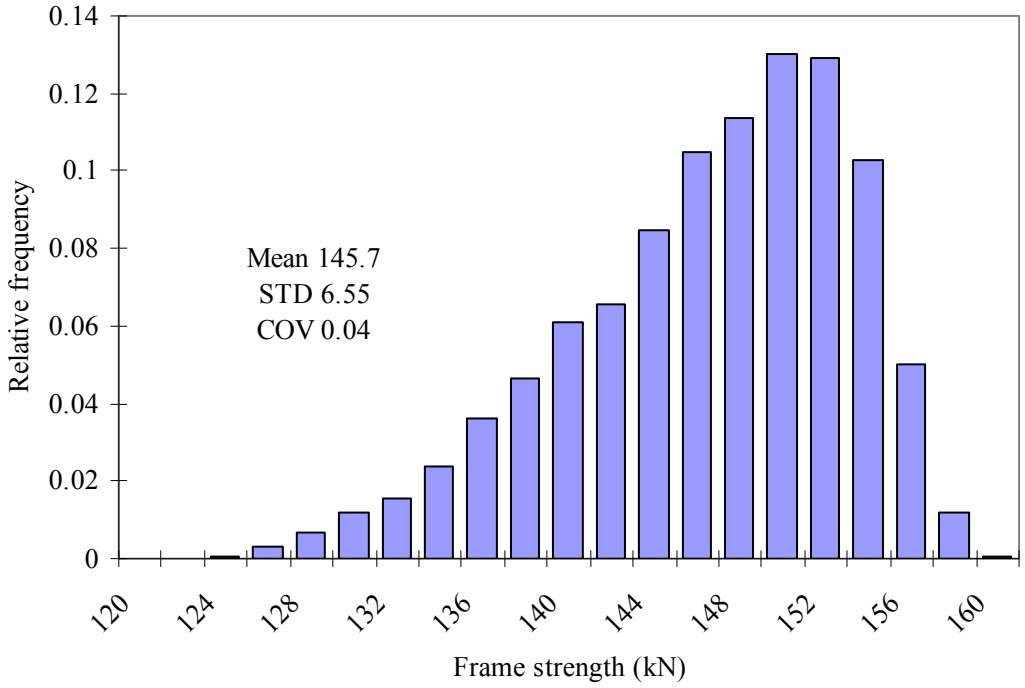

Figure 14: Histogram for the ultimate strength of 3x6 bays, 1 m lift height, 3 lifts, and 300 mm top and bottom jack extensions support scaffold frame

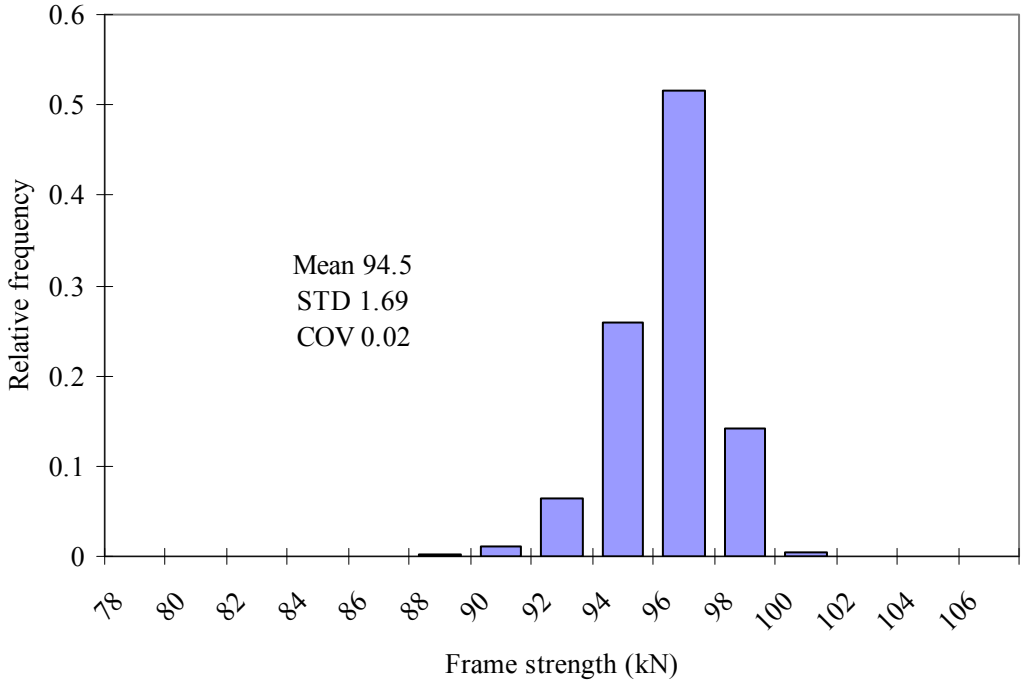

Figure 15: Histogram for the ultimate strength of 3x6 bays, 1 m lift height, 3 lifts, and 600 mm top and bottom jack extensions support scaffold frame

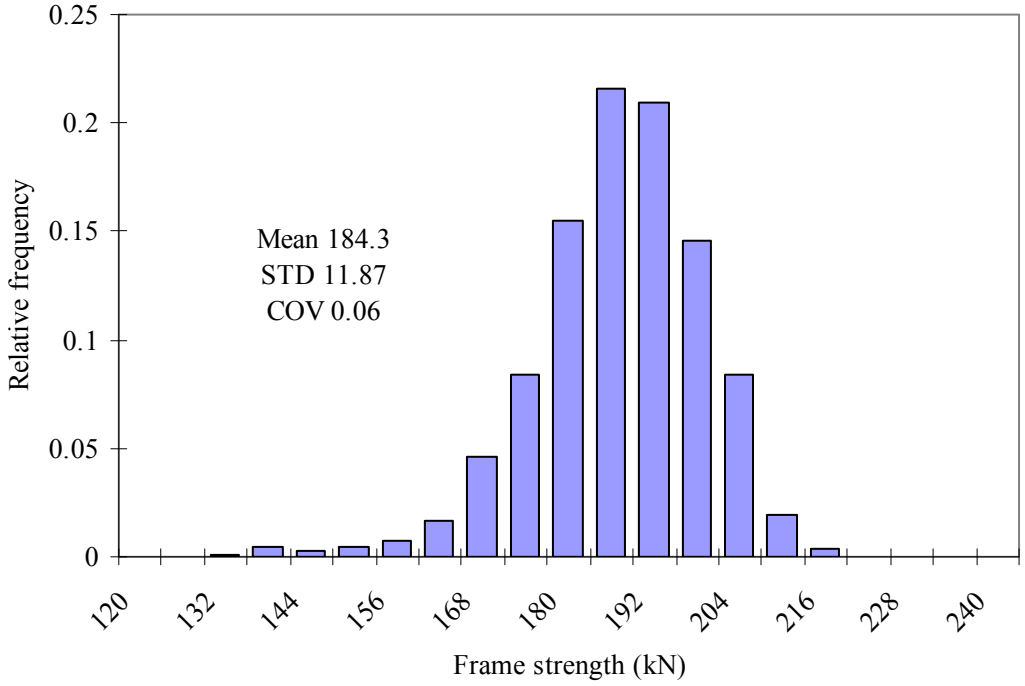

Figure 16: Histogram for the ultimate strength of 9x9 bays, 1 m lift height, 3 lifts, and 100 mm top and bottom jack extensions support scaffold frame

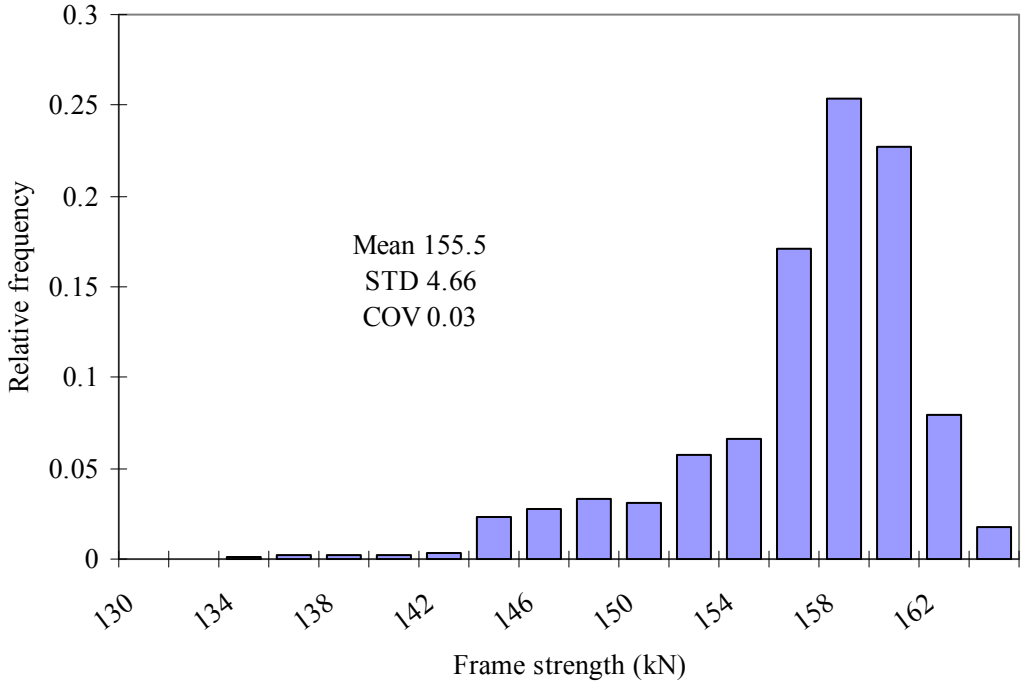

Figure 17: Histogram for the ultimate strength of 9x9 bays, 1 m lift height, 3 lifts, and 300 mm top and bottom jack extensions support scaffold frame

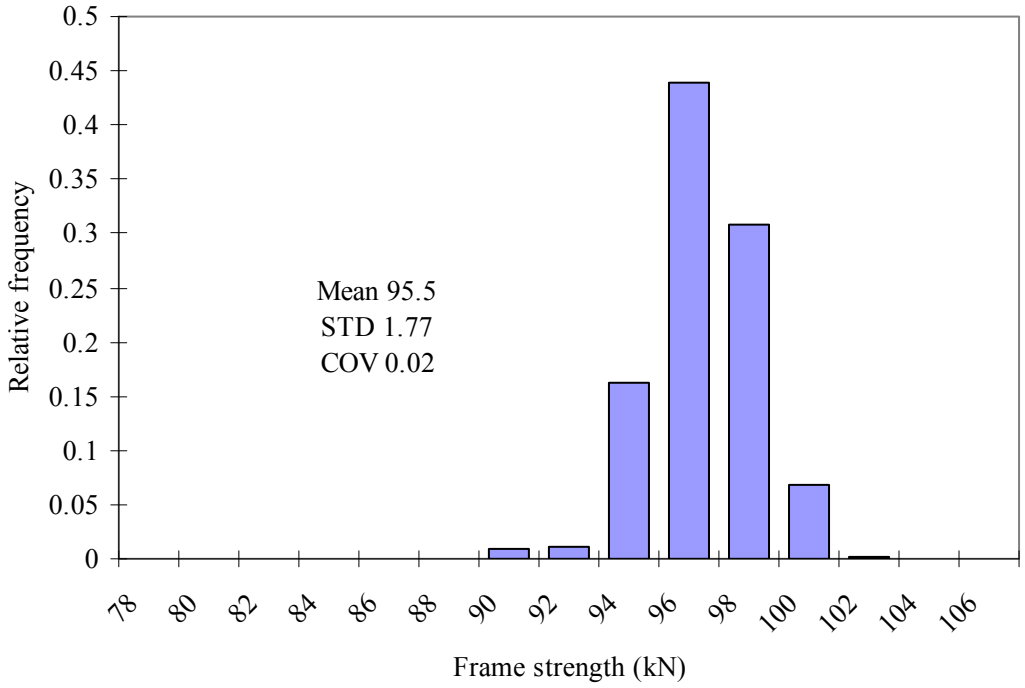

Figure 18: Histogram for the ultimate strength of 9x9 bays, 1 m lift height, 3 lifts, and 600 mm top and bottom jack extensions support scaffold frame

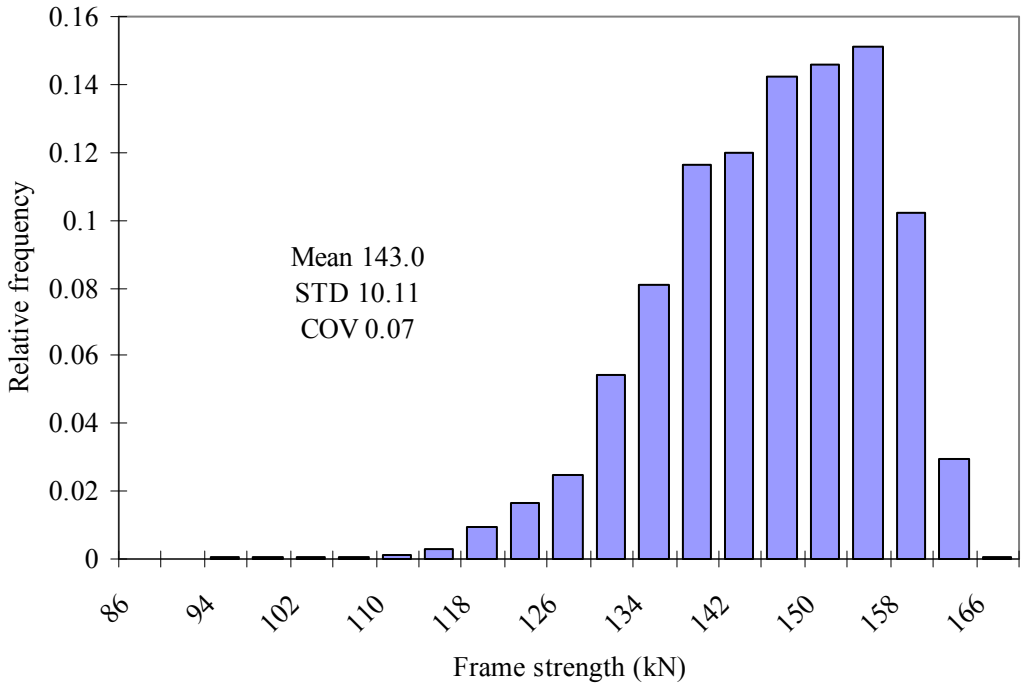

Figure 19: Histogram for the ultimate strength of 1x1 bay, 1.5 m lift height, 3 lifts, and 100 mm top and bottom jack extensions support scaffold frame

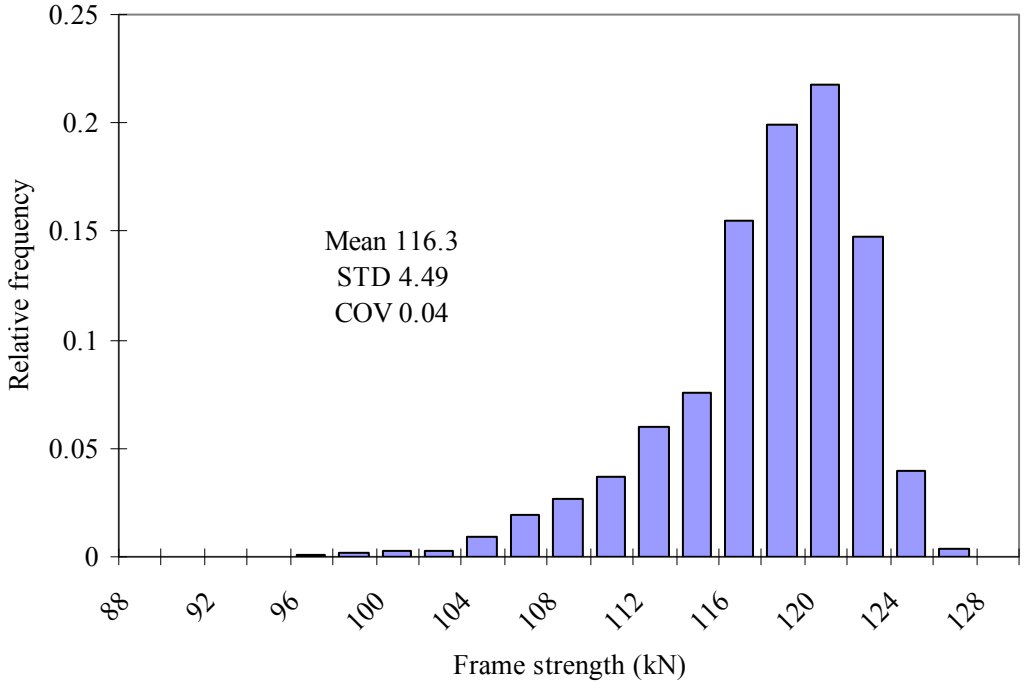

Figure 20: Histogram for the ultimate strength of 1x1 bay, 1.5 m lift height, 3 lifts, and 300 mm top and bottom jack extensions support scaffold frame

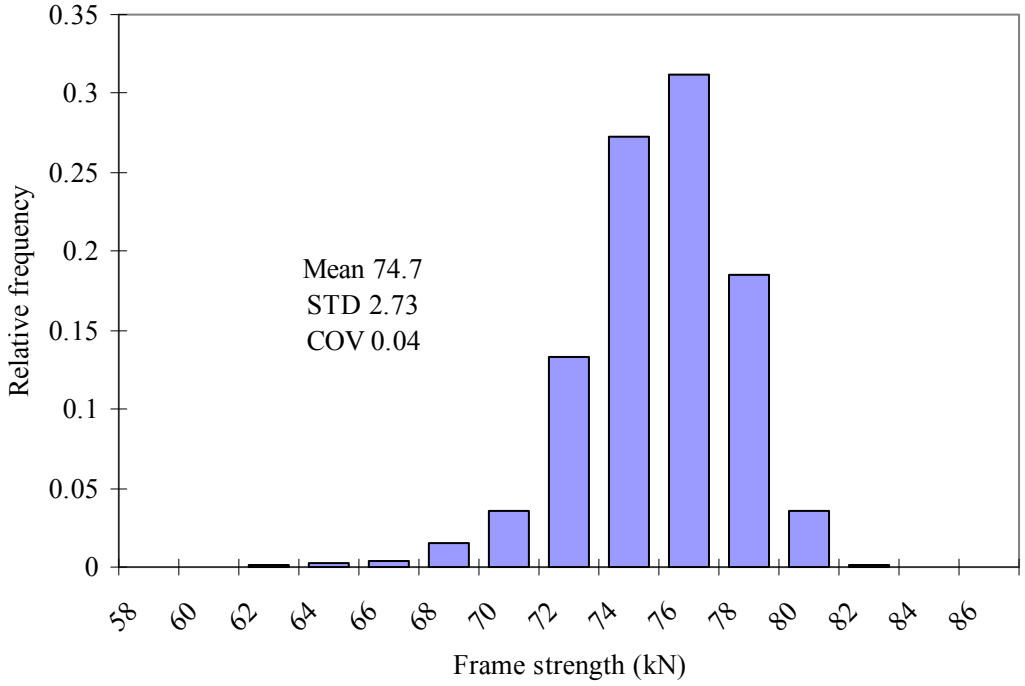

Figure 21: Histogram for the ultimate strength of 1x1 bay, 1.5 m lift height, 3 lifts, and 600 mm top and bottom jack extensions support scaffold frame

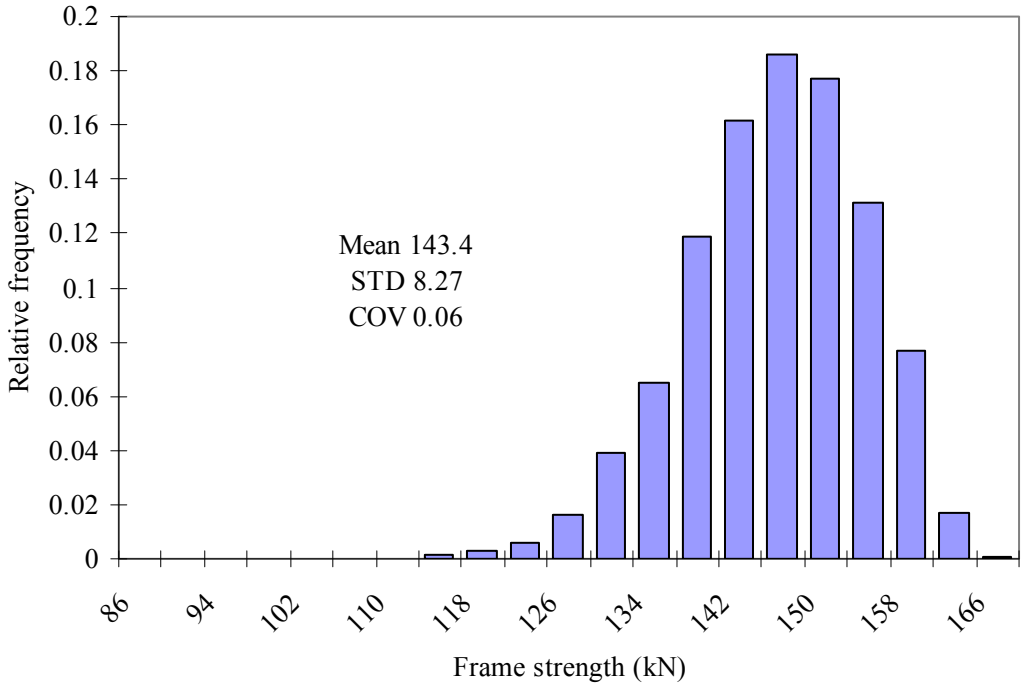

Figure 22: Histogram for the ultimate strength of 3x3 bays, 1.5 m lift height, 3 lifts, and 100 mm top and bottom jack extensions support scaffold frame

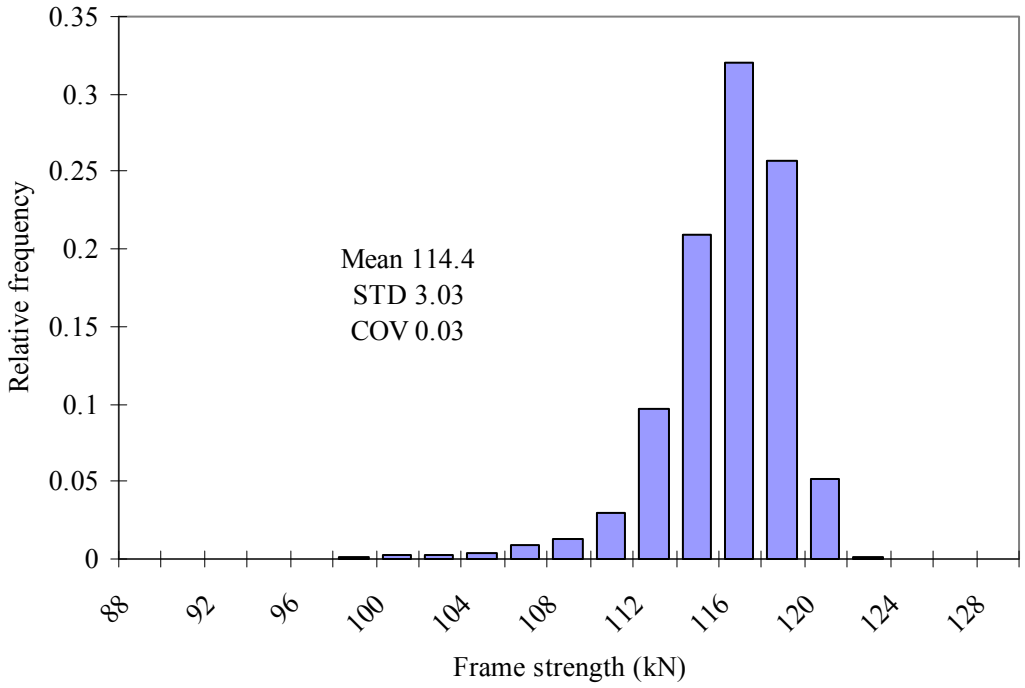

Figure 23: Histogram for the ultimate strength of 3x3 bays, 1.5 m lift height, 3 lifts, and 300 mm top and bottom jack extensions support scaffold frame

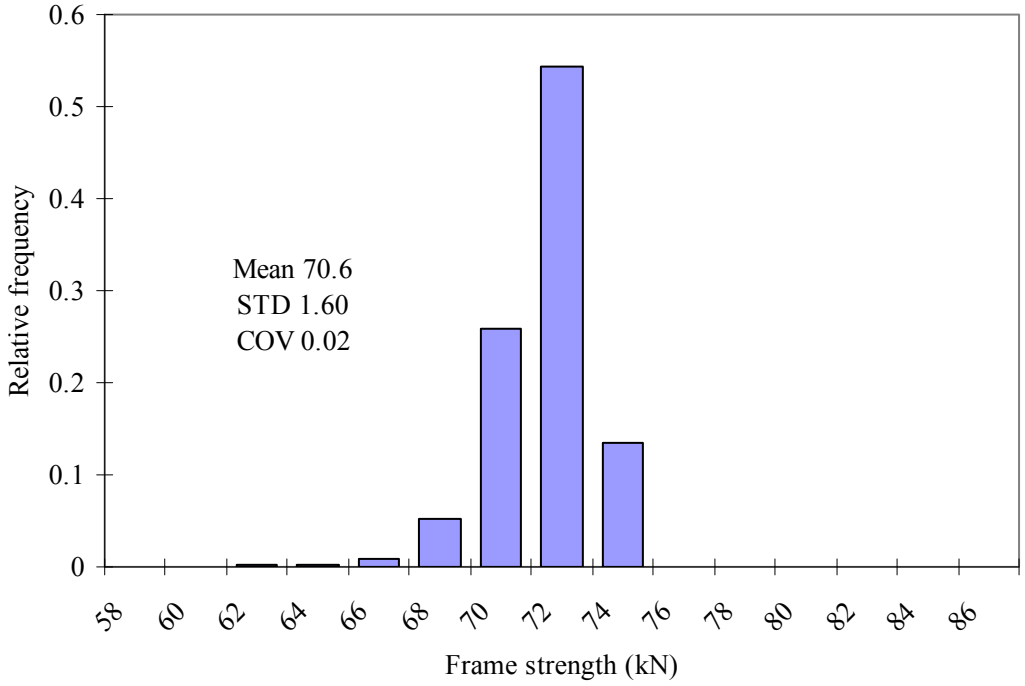

Figure 24: Histogram for the ultimate strength of 3x3 bays, 1.5 m lift height, 3 lifts, and 600 mm top and bottom jack extensions support scaffold frame

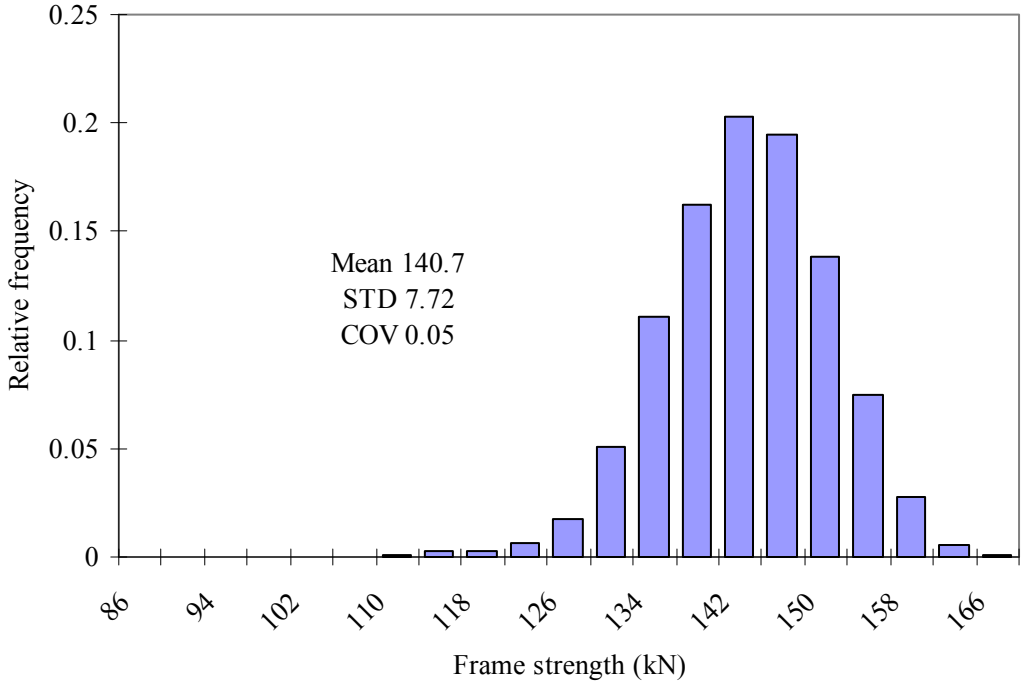

Figure 25: Histogram for the ultimate strength of 3x6 bays, 1.5 m lift height, 3 lifts, and 100 mm top and bottom jack extensions support scaffold frame

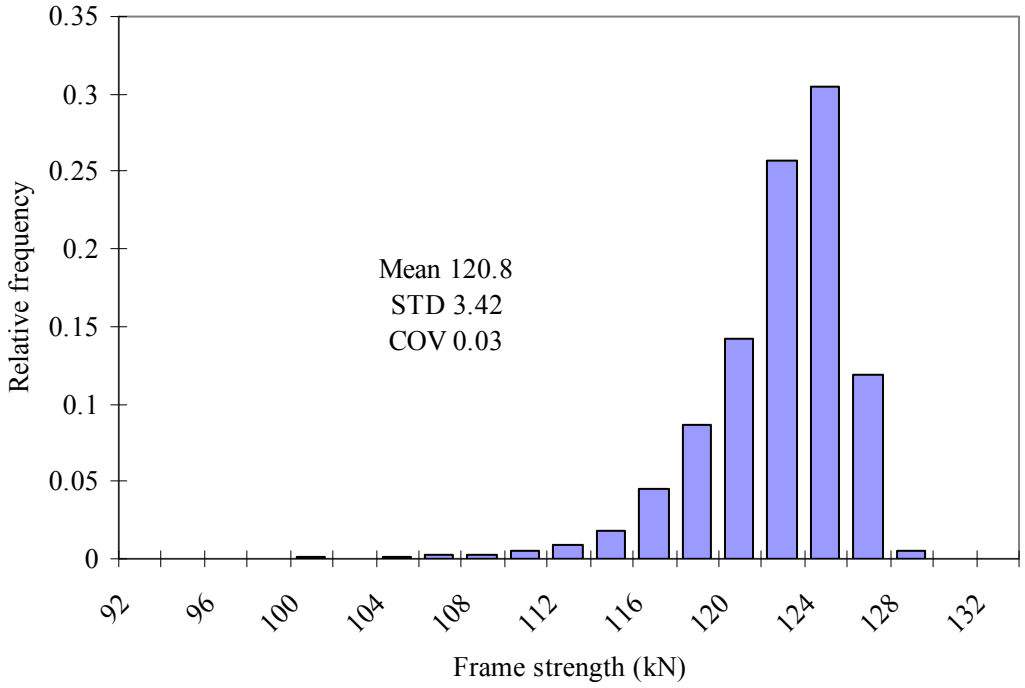

Figure 26: Histogram for the ultimate strength of 3x6 bays, 1.5 m lift height, 3 lifts, and 300 mm top and bottom jack extensions support scaffold frame

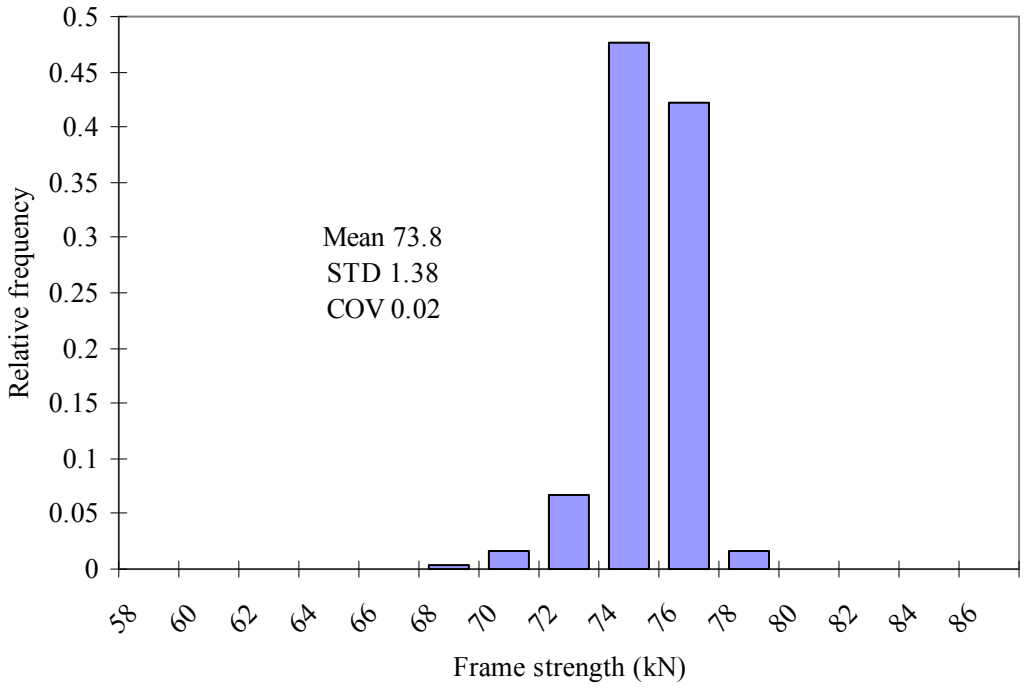

Figure 27: Histogram for the ultimate strength of 3x6 bays, 1.5 m lift height, 3 lifts, and 600 mm top and bottom jack extensions support scaffold frame

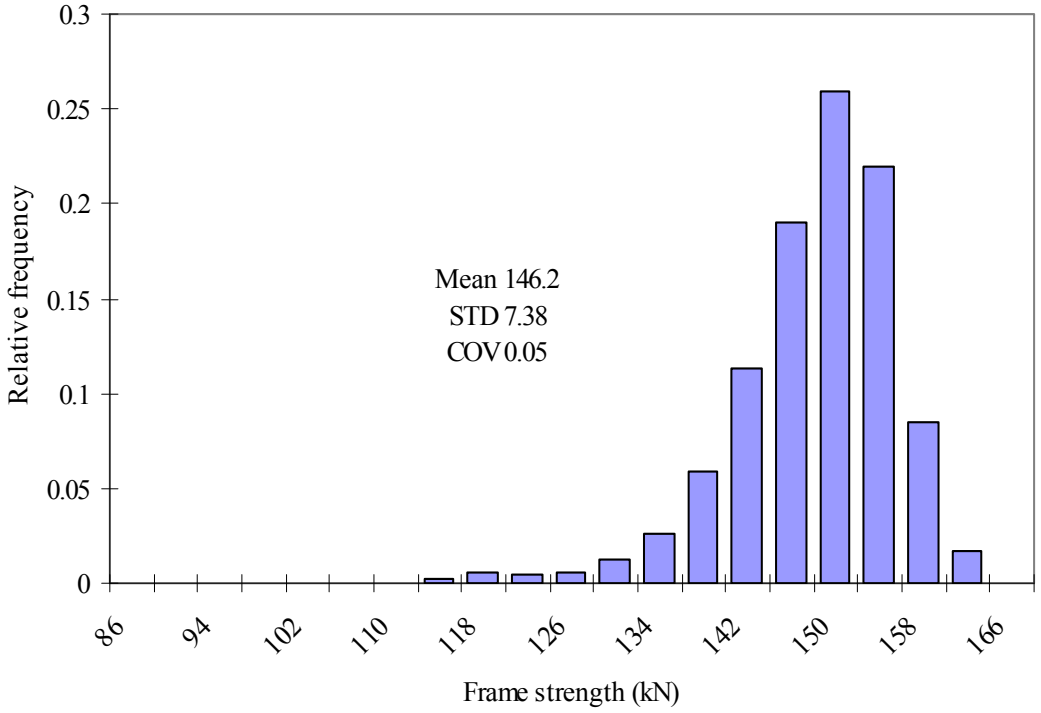

Figure 28: Histogram for the ultimate strength of 9x9 bays, 1.5 m lift height, 3 lifts, and 100 mm top and bottom jack extensions support scaffold frame

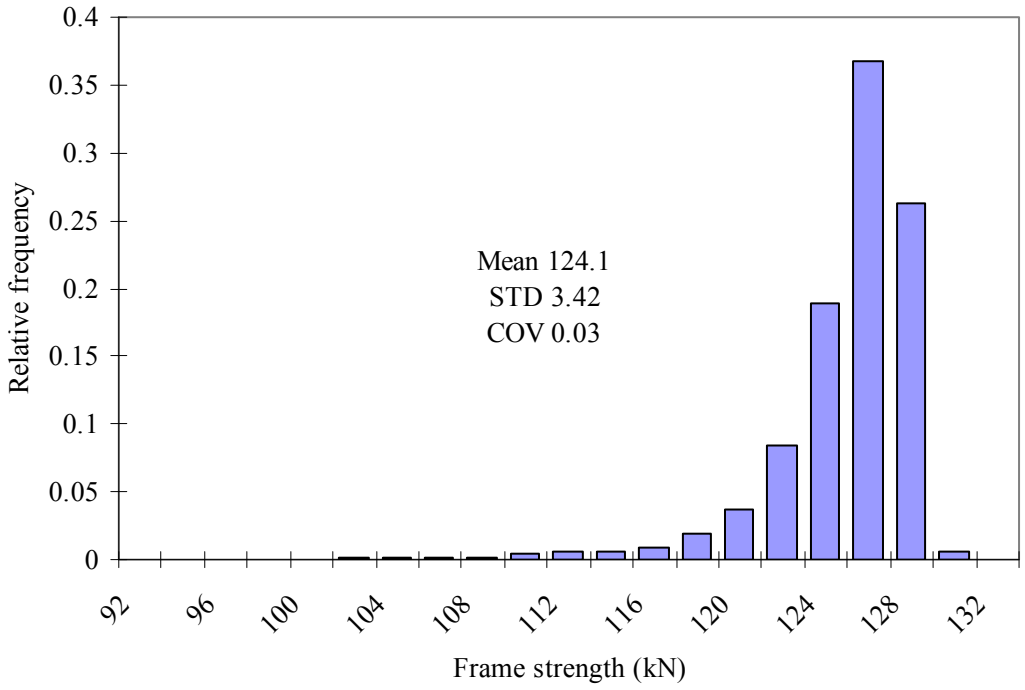

Figure 29: Histogram for the ultimate strength of 9x9 bays, 1.5 m lift height, 3 lifts, and 300 mm top and bottom jack extensions support scaffold frame

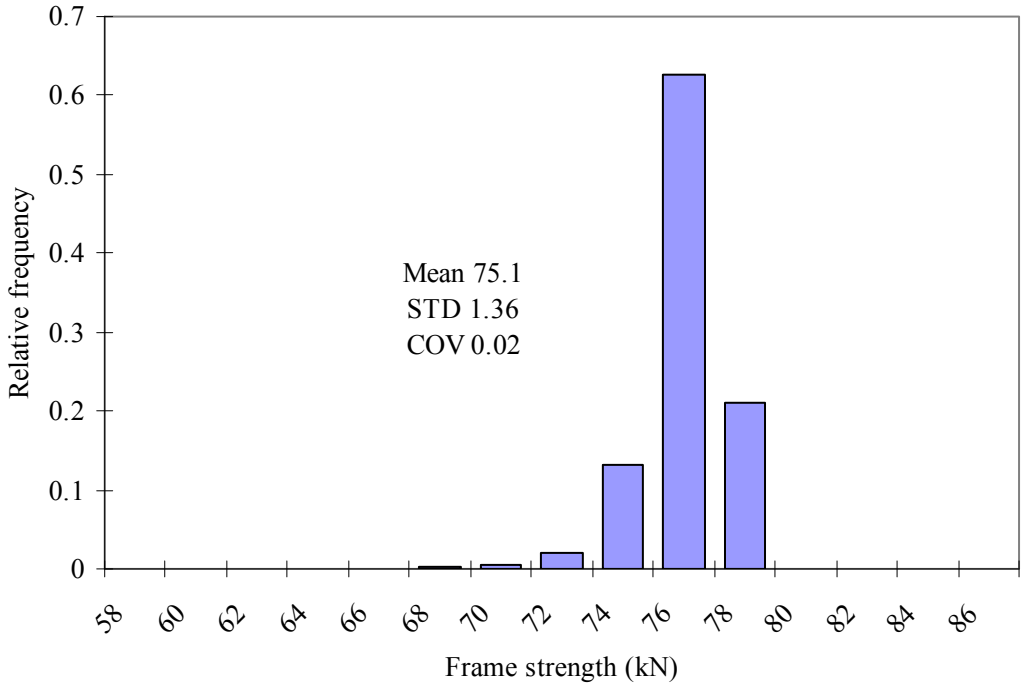

Figure 30: Histogram for the ultimate strength of 9x9 bays, 1.5 m lift height, 3 lifts, and 600 mm top and bottom jack extensions support scaffold frame

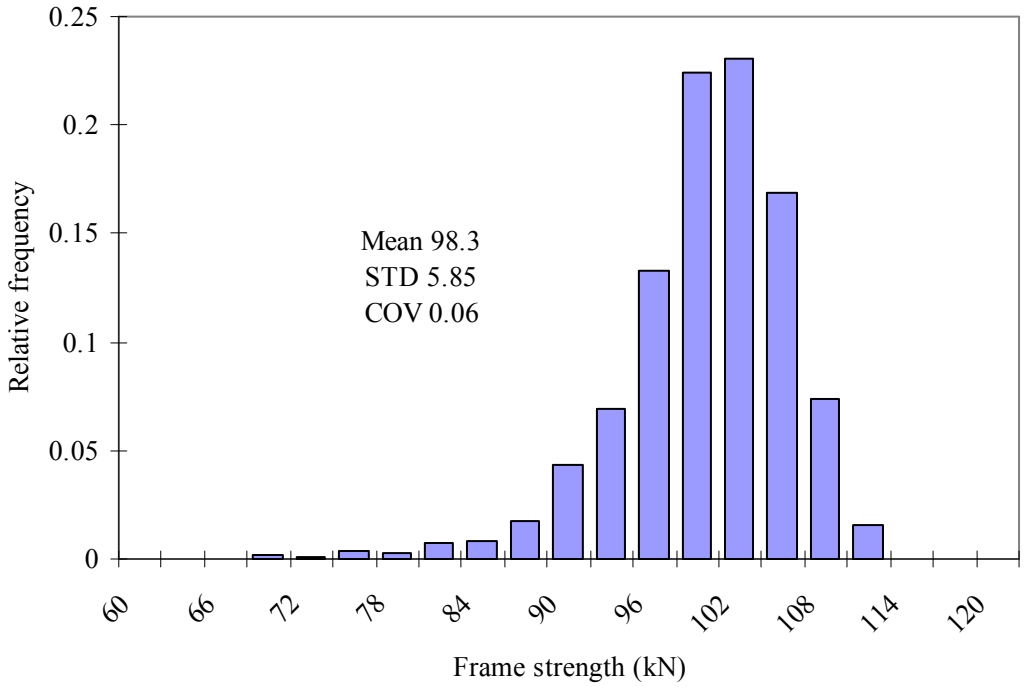

Figure 31: Histogram for the ultimate strength of 1x1 bay, 2 m lift height, 3 lifts, and 100 mm top and bottom jack extensions support scaffold frame

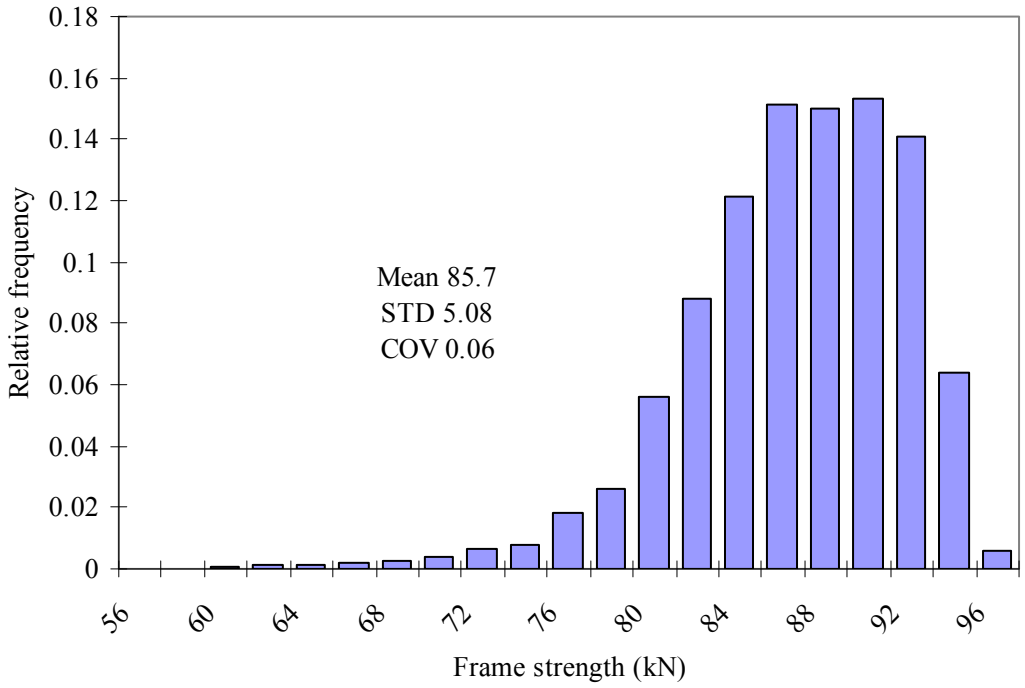

Figure 32: Histogram for the ultimate strength of 1x1 bay, 2 m lift height, 3 lifts, and 300 mm top and bottom jack extensions support scaffold frame

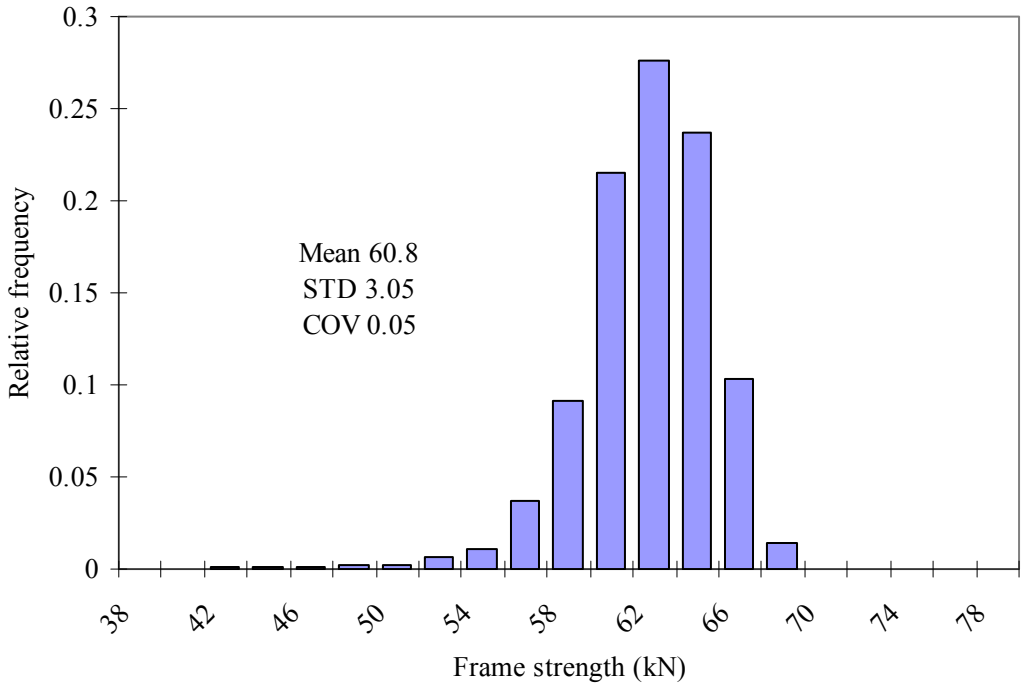

Figure 33: Histogram for the ultimate strength of 1x1 bay, 2 m lift height, 3 lifts, and 600 mm top and bottom jack extensions support scaffold frame

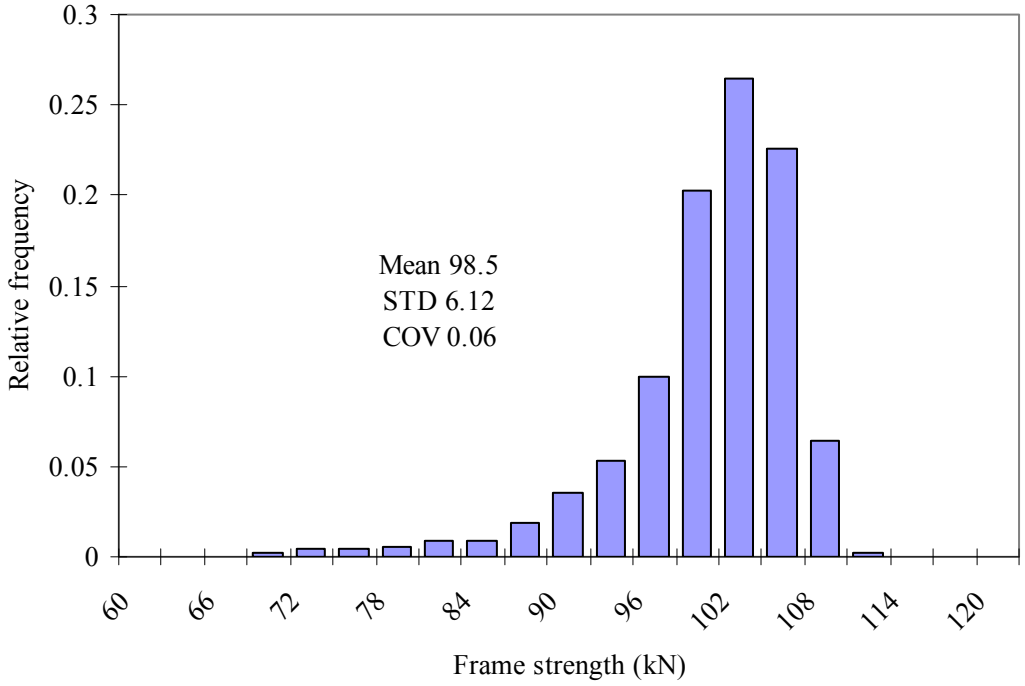

Figure 34: Histogram for the ultimate strength of 3x3 bays, 2 m lift height, 3 lifts, and 100 mm top and bottom jack extensions support scaffold frame

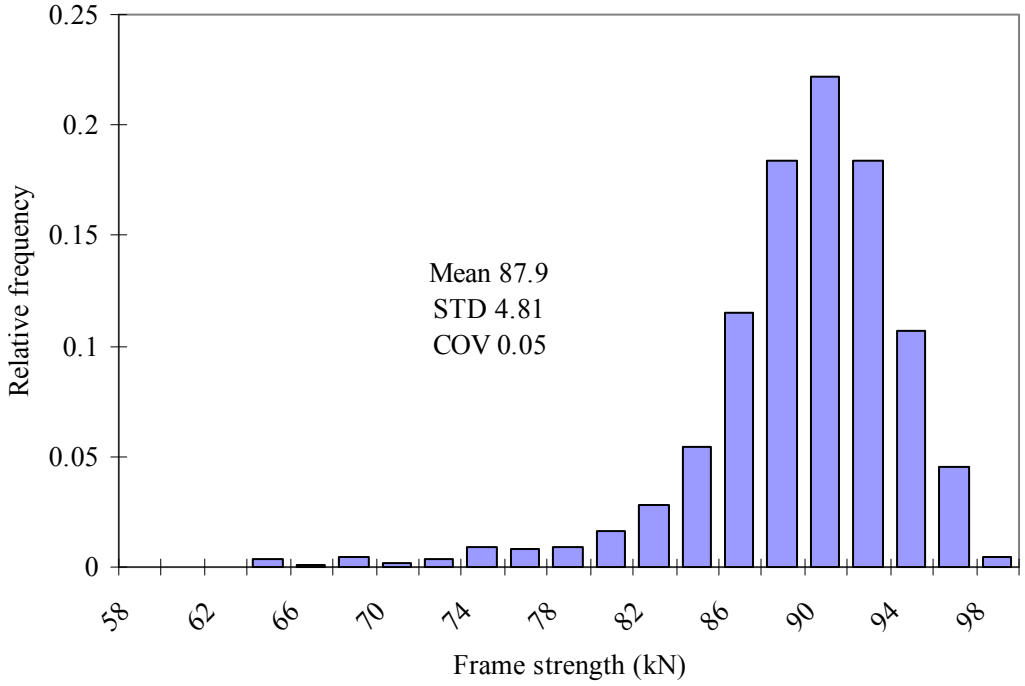

Figure 35: Histogram for the ultimate strength of 3x3 bays, 2 m lift height, 3 lifts, and 300 mm top and bottom jack extensions support scaffold frame

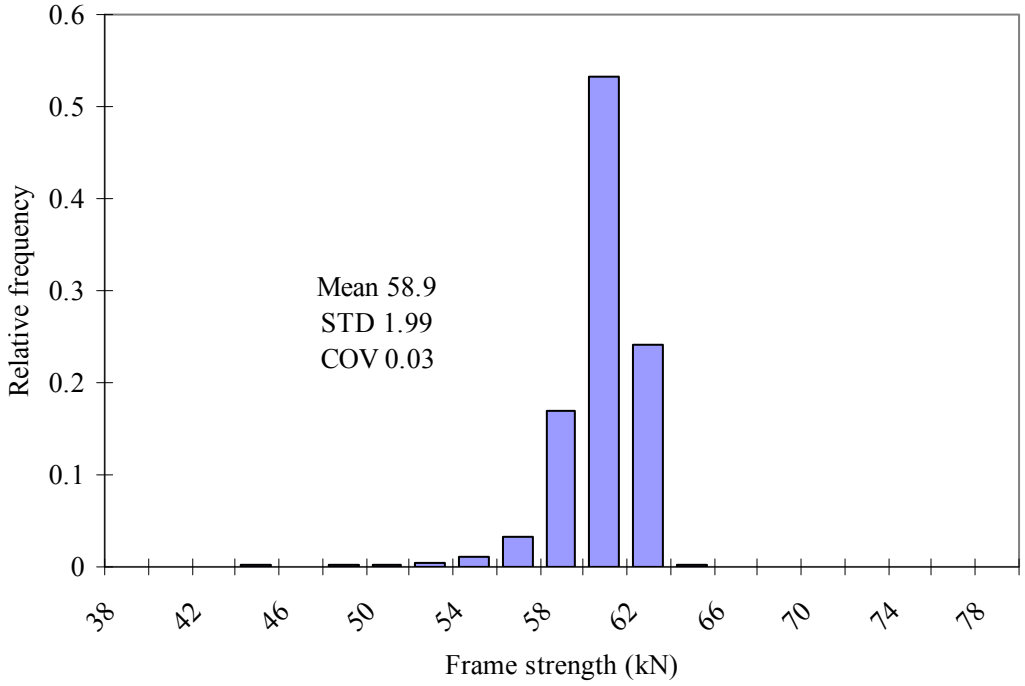

Figure 36: Histogram for the ultimate strength of 3x3 bays, 2 m lift height, 3 lifts, and 600 mm top and bottom jack extensions support scaffold frame

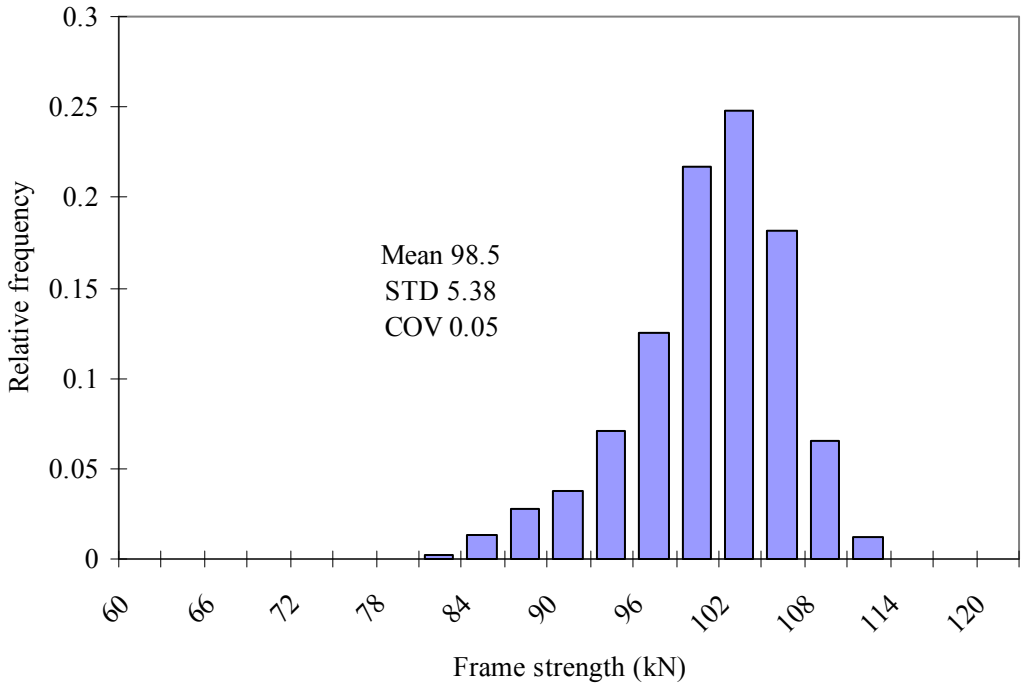

Figure 37: Histogram for the ultimate strength of 3x6 bays, 2 m lift height, 3 lifts, and 100 mm top and bottom jack extensions support scaffold frame

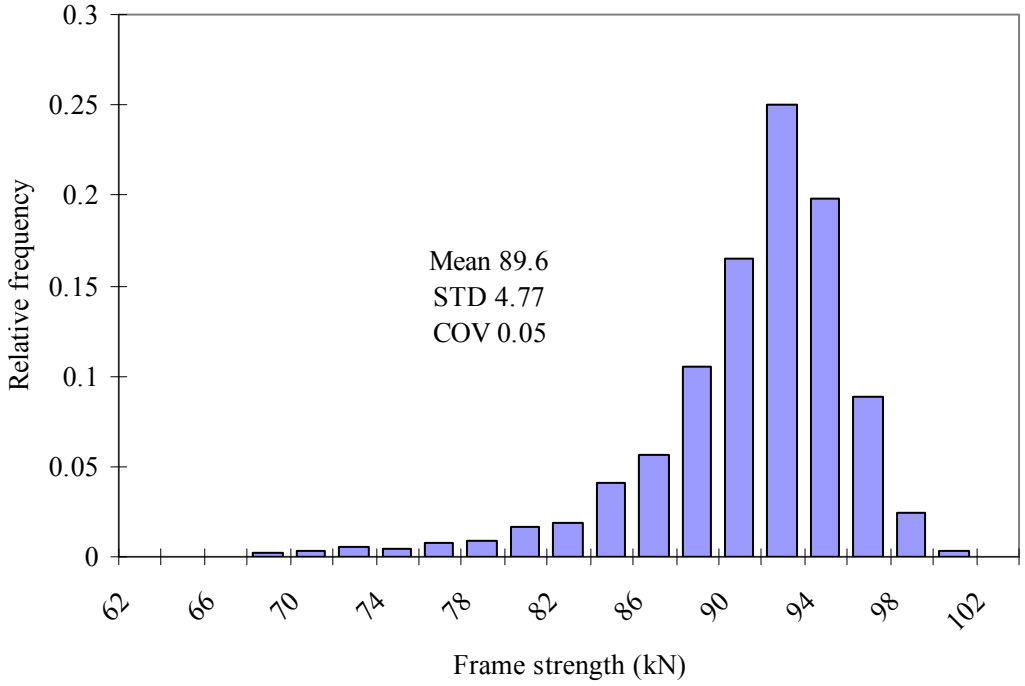

Figure 38: Histogram for the ultimate strength of 3x6 bays, 2 m lift height, 3 lifts, and 300 mm top and bottom jack extensions support scaffold frame

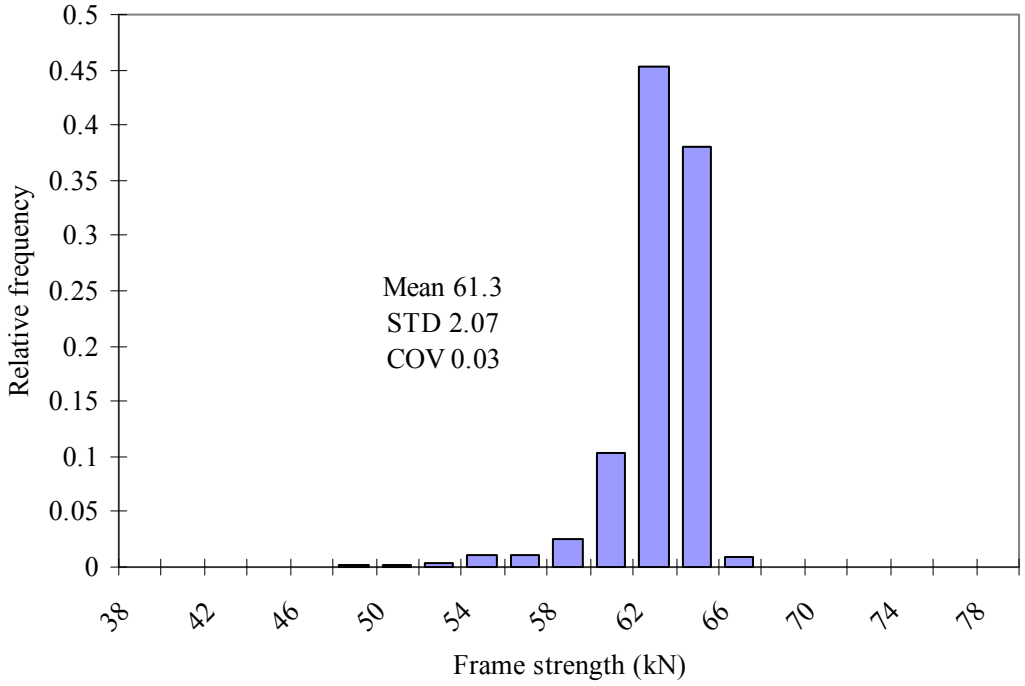

Figure 39: Histogram for the ultimate strength of 3x6 bays, 2 m lift height, 3 lifts, and 600 mm top and bottom jack extensions support scaffold frame

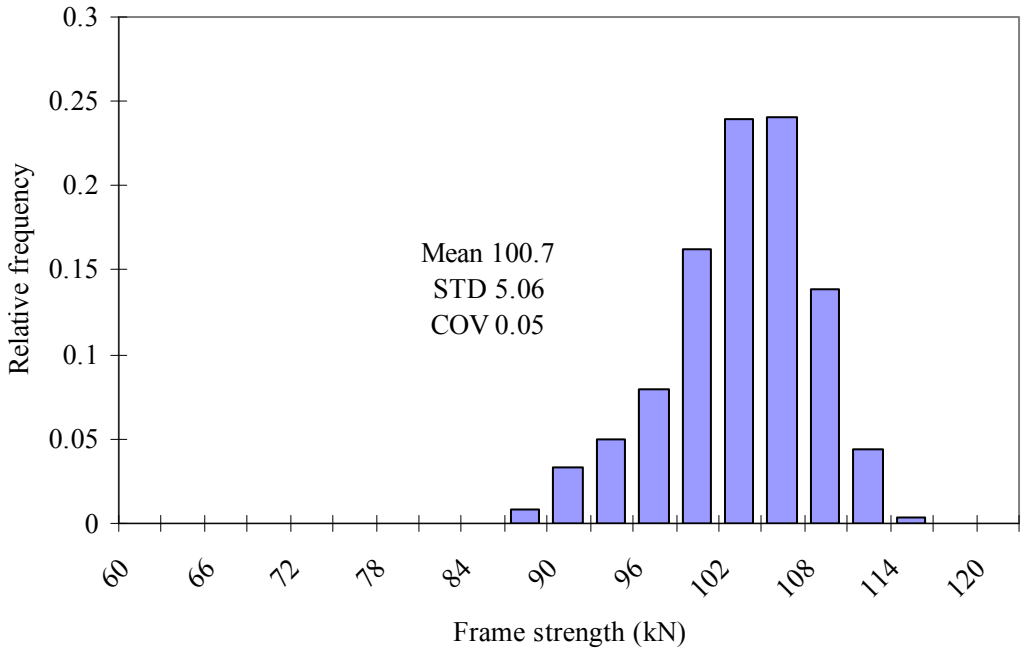

Figure 40: Histogram for the ultimate strength of 9x9 bays, 2 m lift height, 3 lifts, and 100 mm top and bottom jack extensions support scaffold frame

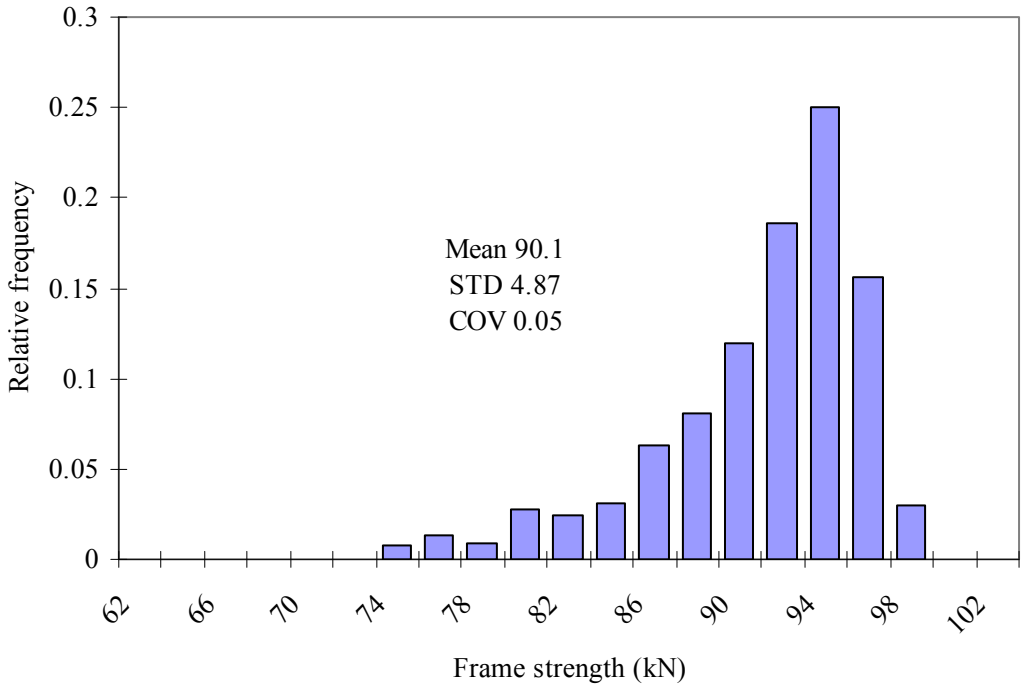

Figure 41: Histogram for the ultimate strength of 9x9 bays, 2 m lift height, 3 lifts, and 300 mm top and bottom jack extensions support scaffold frame

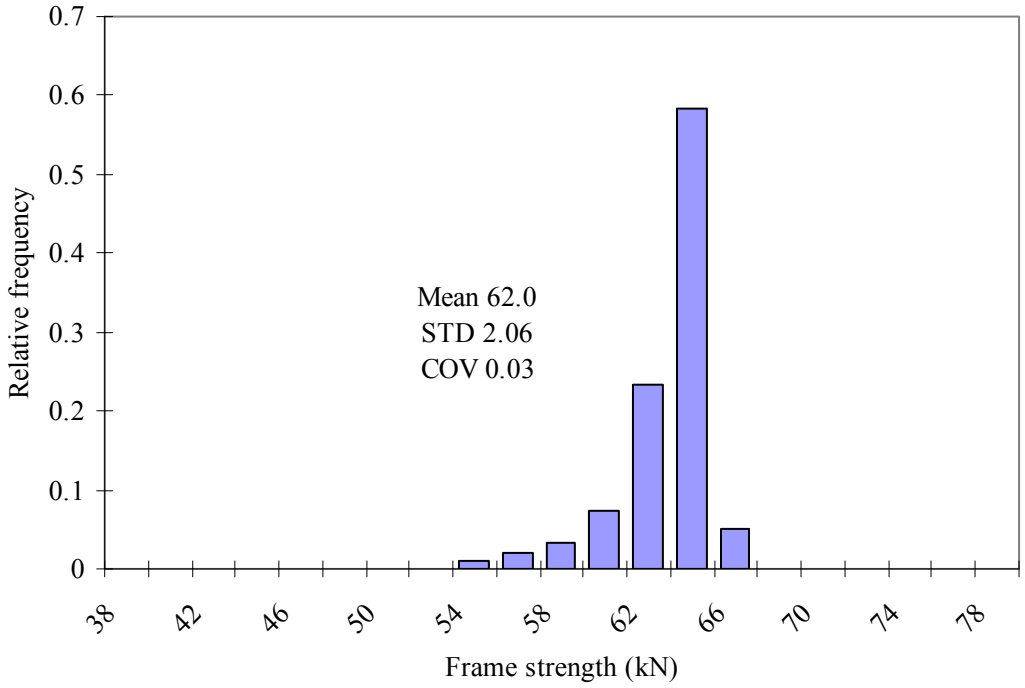

Figure 42: Histogram for the ultimate strength of 9x9 bays, 2 m lift height, 3 lifts, and 600 mm top and bottom jack extensions support scaffold frame

Table 6: Statistical summary of simulation results for system ultimate strengths

Lift height (m)	Jack extensions (mm)	Number of lifts	Number of bays	$\overline{R}$ (kN)	V_R
1.0	100	3	1x1	188.2	0.11
1.0	300	3	1x1	148.7	0.05
1.0	600	3	1x1	94.0	0.03
1.0	100	3	3x3	181.1	0.07
1.0	300	3	3x3	141.9	0.03
1.0	600	3	3x3	90.7	0.03
1.0	100	3	3x6	184.5	0.06
1.0	300	3	3x6	145.7	0.04
1.0	600	3	3x6	94.5	0.02
1.0	100	3	9x9	184.3	0.06
1.0	300	3	9x9	155.5	0.03

Lift height (m)	Jack extensions (mm)	Number of lifts	Number of bays	$\overline{R}$ (kN)	V_R
1.0	600	3	9x9	95.5	0.02
1.5	100	3	1x1	143.0	0.07
1.5	300	3	1x1	116.3	0.04
1.5	600	3	1x1	74.7	0.04
1.5	100	3	3x3	143.4	0.06
1.5	300	3	3x3	114.4	0.03
1.5	600	3	3x3	70.6	0.02
1.5	100	3	3x6	140.7	0.05
1.5	300	3	3x6	120.8	0.03
1.5	600	3	3x6	73.8	0.02
1.5	100	3	9x9	146.2	0.05
1.5	300	3	9x9	124.1	0.03
1.5	600	3	9x9	75.1	0.02
2.0	100	3	1x1	98.3	0.06
2.0	300	3	1x1	85.7	0.06
2.0	600	3	1x1	60.8	0.05
2.0	100	3	3x3	98.5	0.06
2.0	300	3	3x3	87.9	0.05
2.0	600	3	3x3	58.9	0.03
2.0	100	3	3x6	98.5	0.05
2.0	300	3	3x6	89.6	0.05
2.0	600	3	3x6	61.3	0.03
2.0	100	3	9x9	100.7	0.05
2.0	300	3	9x9	90.1	0.05
2.0	600	3	9x9	62.0	0.03

The histograms are shown to be skewed to the left and appear more scattered when the jack extension becomes shorter, resulting in higher coefficients of variation. Also, with shorter lift height, the COV appears to be larger. These results could be expected since with shorter lift height and jack extension, the nonlinear material effects become more pronounced, and hence the variation in yield stress becomes a main controlling factor, which added to other uncertainties, would lead to higher variability in system strength. This assertion has been confirmed by the stress and strain results obtained at the ultimate load in the advanced analysis of the systems with 1 m lift height or 100 mm jack extension, which show that the stress and strain of the standards and jacks are in the plastic region at ultimate. On the other hand, for the systems with 2 m lift or 600 mm jack extension, the ultimate stress and strain results are still in the elastic range and the failure of these systems occurs essentially by elastic buckling. Figures 43 and 44 show typical failure modes and stresses at the ultimate loads of the 1 m lift and 2 m lift systems, respectively. According to the results with similar lift height and jack extension, the mean strength increases by a small amount when the system becomes larger from 3x3 bays to 9x9 bays; however, with the 1x1 bay system, the mean strength can show somewhat higher value than that of the 3x3 bays with the same lift height and jack extensions, since the system with 3x3 bays does not have braces at the corners which can weaken the system strength. In all cases, the variability (COV) of the systems with the same lift height and jack extensions decreases when the system becomes larger due to the structural redundancy and stochastic averaging of uncorrelated member properties.

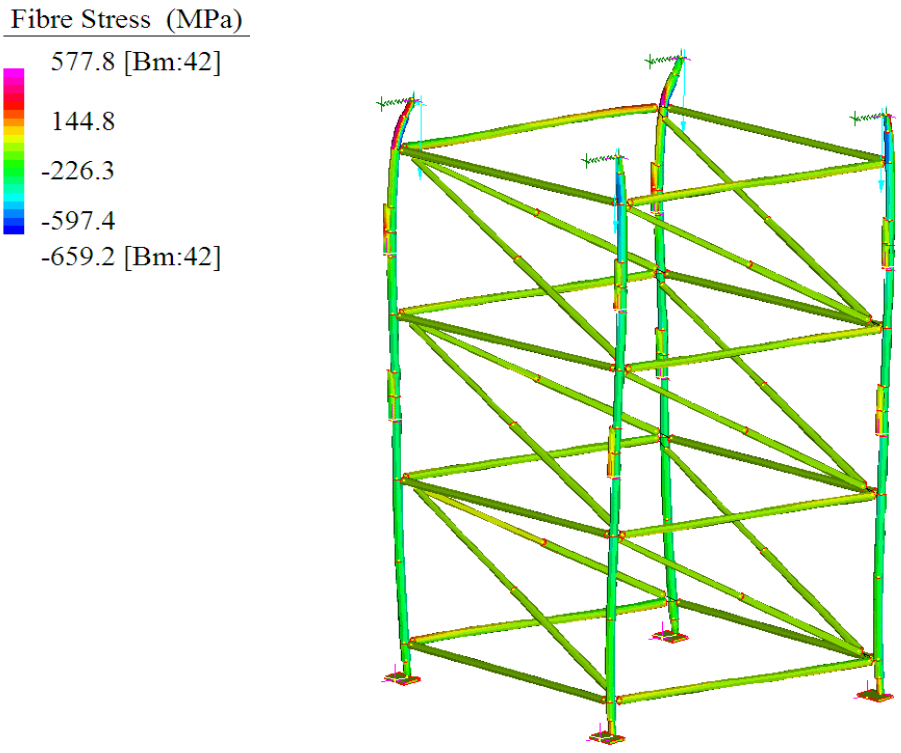

Figure 43: Typical failure mode of 1.0 m lift system with 100 mm jack extensions

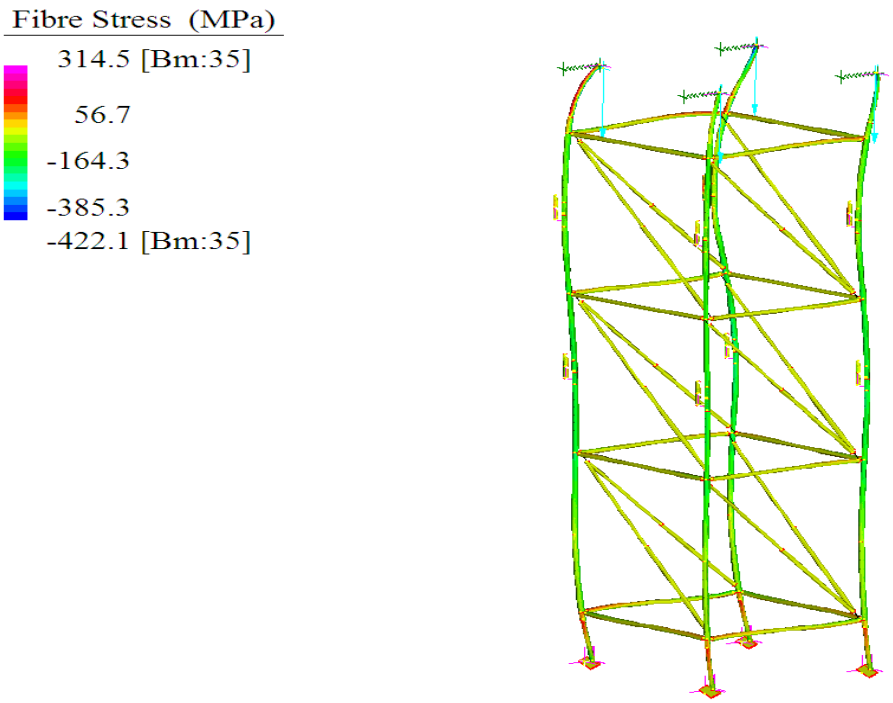

Figure 44: Typical failure mode of 2.0 m lift system with 600 mm jack extensions

4.2 NOMINAL DESIGN MODELS

The nominal design models are created in the same way as the analysis models, except that all inputs are applied at nominal or proposed values and all material models are assumed to be elastic-perfectly plastic (Figure 45) at the nominal yield stress (f_y). The pattern of geometric imperfections and loading eccentricity is set to be at the worst case scenario, i.e. first buckling mode shape. These nominal models are intended for engineers to use in practice when designing scaffold systems by advanced analysis. The input parameters for the nominal design models are presented in Table 7. Thirty six nominal design models for the system configurations analysed in the simulations presented in Section 4.1 were analysed by advanced analyses to obtain the nominal ultimate strength (R_n) for each. The results are shown in Table 8.

Table 7: Input parameters for nominal design models

Parameter	Nominal value	Description
Storey out-of-plumb	H/600	H = height of the system
Out-of-straightness of the standards	L_h/700	L_h = lift height
Loading eccentricity	19 mm	Mean value from survey
Bottom eccentricity	15 mm	See Section 3.5

Parameter	Nominal value	Description
Section properties	Nominal	See Section 2
Joint stiffness	Mean	See Tables 1 and 2
Yield stress for the standard	450 MPa	Nominal steel grades (see Figure 45 for elastic-perfectly plastic material model)
Yield stress for the jack	430 MPa	
Yield stress for the spigot	400 MPa	
Yield stress for the ledger	350 MPa	
Yield stress for the brace	400 MPa	
Yield stress for the base plate	250 MPa	

Table 8: Nominal ultimate strength for nominal design models

Lift height (m)	Jack extensions (mm)	Number of lifts	Number of bays	R_n (kN)
1.0	100	3	1x1	141.0
1.0	300	3	1x1	126.3
1.0	600	3	1x1	87.7
1.0	100	3	3x3	137.0
1.0	300	3	3x3	119.3
1.0	600	3	3x3	83.0
1.0	100	3	3x6	137.0
1.0	300	3	3x6	119.3
1.0	600	3	3x6	83.0
1.0	100	3	9x9	140.0
1.0	300	3	9x9	122.0
1.0	600	3	9x9	87.0
1.5	100	3	1x1	121.7
1.5	300	3	1x1	106.0

Lift height (m)	Jack extensions (mm)	Number of lifts	Number of bays	R_n (kN)
1.5	600	3	1x1	70.2
1.5	100	3	3x3	120.2
1.5	300	3	3x3	107.5
1.5	600	3	3x3	69.0
1.5	100	3	3x6	119.9
1.5	300	3	3x6	107.7
1.5	600	3	3x6	71.0
1.5	100	3	9x9	124.1
1.5	300	3	9x9	116.2
1.5	600	3	9x9	74.1
2.0	100	3	1x1	87.7
2.0	300	3	1x1	77.0
2.0	600	3	1x1	56.5
2.0	100	3	3x3	88.7
2.0	300	3	3x3	80.5
2.0	600	3	3x3	57.0
2.0	100	3	3x6	88.8
2.0	300	3	3x6	81.3
2.0	600	3	3x6	59.5
2.0	100	3	9x9	91.0
2.0	300	3	9x9	83.5
2.0	600	3	9x9	61.2

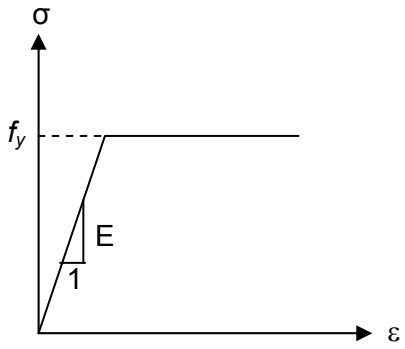

Figure 45: Elastic-perfectly plastic model for steel

4.3 MODELLING UNCERTAINTY AND STATISTICS OF SYSTEM RESISTANCE

As mentioned in Section 3, the Monte Carlo simulations consider only the inherent randomness in basic variables, often referred to as aleatory in structural engineering, which relates to luck or chance (Ayyub and McCuen 2003; Bulleit 2008). Another type of uncertainty, which arises from simplifications and assumptions in the modelling of support scaffold systems, must also be accounted for in the reliability analysis in order to develop probabilistic-based design by advanced analysis. This source of uncertainty, also called epistemic or modelling error, includes simplified boundary conditions, modelised initial geometric imperfections, idealised moment-rotation curves for joint stiffness, and inherent inaccuracy in the discretisation of the structure into a finite element model. The mean error and coefficient of variation (COV) of the advanced analysis model can be obtained from the ratios of fifteen comparisons presented in Chandrangsu and Rasmussen (2009b) between the measured ultimate loads (R_{test}) and the ultimate load predictions from advanced analysis ($R_{predict}$). The mean error is 1.014 with a COV of 0.1 (Chandrangsu and Rasmussen 2009b), suggesting that the advanced analysis of finite element models proposed in this research provides good indication of the true system strength. The variability of $R_{test} / R_{predict}$ ($V_{test/predict}$) comes from three causes (Ellingwood et al. 1980), as explained by:

$$V_{test\,/\,predict}^2 = V_M^2 + V_T^2 + V_S^2 \tag{1}$$

where V_M represents the modelling uncertainty, V_T represents the uncertainties in testing procedures and readings, and V_S represents the variations in test environments and actual test specimen dimensions from those measured. In general, V_T and V_S are in the range of 0.02-0.04 for members (Melchers 1999). For the structural system studied herein, the effects from V_T and V_S are difficult to quantify, and are conservatively ignored, thus taking V_M equal to $V_{test/predict}$. To incorporate the effect of modelling error, the predicted ultimate load result from each Monte Carlo simulation for the same system configuration is modified by multiplying the ultimate load by a randomly generated value of modelling error, which is assumed to be normally distributed with a mean of 1.014 and a COV of 0.1 (Chandrangsu and Rasmussen 2009b). After combining the modelling uncertainty, the statistics for the true system resistance of support scaffold systems are obtained. The mean-

to-nominal ratio or bias factor for system resistance ($\overline{R}/R_n$ or λ_R) and corresponding coefficient of variation (V_R) for each system configuration are presented in Table 9. Since the modelling uncertainty has higher COV than that of simulated strength, the overall variability of system resistance is highly influenced by the modelling error. The lognormal distribution is conservatively assumed as a probabilistic model for the system resistance in the reliability analysis when using the first-order reliability method (FORM).

Table 9: Statistics for the system resistance of support scaffold systems

Lift height (m)	Jack extensions (mm)	Number of bays	$\overline{R}/R_n$	V_R
1.0	100	1x1	1.35	0.15
1.0	300	1x1	1.19	0.11
1.0	600	1x1	1.09	0.10
1.0	100	3x3	1.34	0.12
1.0	300	3x3	1.21	0.10
1.0	600	3x3	1.11	0.10
1.0	100	3x6	1.37	0.12
1.0	300	3x6	1.24	0.11
1.0	600	3x6	1.15	0.10
1.0	100	9x9	1.33	0.12
1.0	300	9x9	1.29	0.10
1.0	600	9x9	1.11	0.10
1.5	100	1x1	1.19	0.12
1.5	300	1x1	1.11	0.11
1.5	600	1x1	1.08	0.11
1.5	100	3x3	1.21	0.12
1.5	300	3x3	1.08	0.10
1.5	600	3x3	1.04	0.10
1.5	100	3x6	1.19	0.11
1.5	300	3x6	1.14	0.10

Lift height (m)	Jack extensions (mm)	Number of bays	$\overline{R} / R_n$	V_R
1.5	600	3x6	1.05	0.10
1.5	100	9x9	1.19	0.11
1.5	300	9x9	1.08	0.10
1.5	600	9x9	1.03	0.10
2.0	100	1x1	1.14	0.12
2.0	300	1x1	1.13	0.12
2.0	600	1x1	1.09	0.11
2.0	100	3x3	1.13	0.12
2.0	300	3x3	1.11	0.11
2.0	600	3x3	1.05	0.10
2.0	100	3x6	1.13	0.11
2.0	300	3x6	1.12	0.11
2.0	600	3x6	1.04	0.10
2.0	100	9x9	1.12	0.11
2.0	300	9x9	1.10	0.11
2.0	600	9x9	1.03	0.10

5 RELIABILITY ANALYSIS WITH DESIGN BY ADVANCED ANALYSIS

The basic structural reliability concept is to find the probability of failure (P_f) of the structure, as defined by:

$$P_f = P(R - Q \le 0) = P(G(R,Q) \le 0) = \int F_R(x)\, f_Q(x) dx \tag{2}$$

in which R is the structural system resistance or system capacity and Q is the total load effect. Both R and Q are modelled as random variables. $G(R, Q)$ represents the limit state function and $G(R,Q) \le 0$ defines the unsafe or failure region. $F_R(x)$ is the cumulative distribution function of R, and $f_Q(x)$ is the probability density function of Q. For practical use in the design by advanced analysis, Eq. (2) is complemented by the familiar LRFD formula, which when applied to a structural system, takes the form:

$$\varphi_{system} R_n \ge \sum \gamma_i Q_i \tag{3}$$

in which R_n is the nominal system resistance determined according to the design procedure (here advanced analysis), Q_i are the nominal design load effects, φ_{system} is the system resistance factor, and γ_i are the load factors. Since the load factors, γ_i, are known and can be set equal to the values in the design standard, then the system resistance factor, φ_{system}, is determined using reliability analysis (FOSM or FORM) to achieve a specific system target reliability index.

In reliability analysis by FOSM, the random variables are assumed to be all normally distributed and uncorrelated. A closed-form FOSM expression for the reliability index β derived in terms of mean-to-nominal values (bias factors) and variances of the random variables, considering only gravity load combination (dead and live loads), can be written as (Melchers 1999):

$$\beta = \frac{\mu_G}{\sigma_G} = \frac{\dfrac{\lambda_R}{\varphi_{system}}\left(\gamma_D + \gamma_L \dfrac{L_n}{D_n}\right)D_n - \lambda_D D_n - \lambda_L\left(\dfrac{L_n}{D_n}\right)D_n}{\sqrt{\left(\dfrac{\lambda_R}{\varphi_{system}}\left(\gamma_D + \gamma_L \dfrac{L_n}{D_n}\right)D_n \times V_R\right)^2 + \left(\lambda_D D_n \times V_D\right)^2 + \left(\lambda_L\left(\dfrac{L_n}{D_n}\right)D_n \times V_L\right)^2}} \tag{4}$$

in which μ_G is the mean value of the limit state function, σ_G is the standard deviation of the limit state function, λ_R is the bias factor for system resistance, λ_D is the bias factor for dead load, λ_L is the bias factor for live load, γ_D is the load factor for dead load, γ_L is the load factor for live load, φ_{system} is the system resistance factor, V_R is the coefficient of variation of system resistance, V_D is the coefficient of variation of dead load, V_L is the coefficient of variation of live load, D_n is the nominal dead load, and L_n is the nominal live load. From Eq. (4), the system resistance factor φ_{system} can be solved for any specified system target reliability β when all other parameters are known.

When the actual distributions of the random variables are taken into account, including distributions which are non-normal, the reliability index can be more accurately approximated using FORM. The FORM analysis is performed in iterative manner. In order to carry out code calibration to obtain φ_{system} with this method, the following step-by-step procedure is used. Again, only the gravity load combination (dead and live loads) is considered in this research.

(a) Formulate the limit state function $G = R - D - L$ where R is system resistance, D is dead load effect, and L is live load effect, and determine the probability distributions with appropriate parameters for all random variables (λ_R, V_R, λ_D, V_D, λ_L, and V_L). For example, assume R is lognormal, D is normal, L is type I extreme value distribution, and L/D = 0.5, (however, when L_n/D_n = 0.5, L/D = 0.4762 is used in Section 5.2, according to the load statistics in Section 5.1).

(b) Obtain an initial design point by assuming $d^* = \mu_D$ and then $l^* = \mu_L = 0.5\mu_D$. Set G = 0, $r^* = 1.5\mu_D$ then using G = 0 evaluate at the mean values, $\mu_R = 1.5\mu_D$.

(c) Determine the equivalent normal parameters for *R* (μ_R^e and σ_R^e) and *L* (μ_L^e and σ_L^e) only since *D* is assumed normal.

(d) Calculate the partial derivatives of the limit state function with respect to the reduced variates and define a column vector $G_{partial}$ (Nowak and Collins 2000).

(e) Calculate a column vector of the sensitivity factors *α* for *R*, *D* and *L* (Nowak and Collins 2000).

(f) Choose a value for the target reliability index *β*.

(g) Find a new design point in reduced variates for *n* – 1 = 2 variables. Choosing the variables for *D* and *L*, then $z_D^* = \alpha_D \beta$ and $z_L^* = \alpha_L \beta$.

(h) Compute the values of corresponding design point in original coordinates for *D* and *L*, then $d^* = \mu_D + z_D^* \sigma_D$ and $l^* = \mu_L^e + z_L^* \sigma_L^e$.

(i) Solve for the value of the remaining random variable *R* by setting the limit state function *G* = 0, then $r^* = d^* + l^*$ and update the mean value of *R* as $\mu_R = \dfrac{r^*}{1 + \alpha_R \beta V_R}$.

(j) Repeat steps (b) to (i) with successive new design points until the design points converge.

(k) Choose load factors: γ_D and γ_L.

(l) Compute system resistance factor as $\varphi_{system} = \dfrac{\gamma_D \left(\dfrac{\mu_D}{\lambda_D} \right) + \gamma_L \left(\dfrac{\mu_L}{\lambda_L} \right)}{\dfrac{\mu_R}{\lambda_R}}$ from Eq. (3).

More information on the code calibration procedure by FOSM and FORM can be found in Melchers (1999) and Nowak and Collins (2000).

5.1 LOAD STATISTICS

Steel support scaffold systems are normally designed to withstand both gravity and wind loads. In the case of wind loads, the top of the support scaffold systems consists of formwork that is usually tied or braced to permanent structures such as lift cores and columns, thus transferring most of the lateral loads into the permanent structures. Also, some of the lateral loads are resisted by the braces on the scaffold systems. The design of support scaffold systems is therefore normally governed by gravity loads from formwork, steel reinforcement, wet concrete, equipment, workers, and stacked materials. In this research, only the gravity load combination of live and dead loads is considered as $1.2D_n+1.6L_n$ and $1.25D_n+1.5L_n$, where D_n is nominal dead load and L_n is nominal live load, based on the minimum design loads proposed by ASCE (2005) and Standard Australia (1995), respectively. The construction dead loads generally consist of the self-weight of concrete, reinforcement, and formwork. In this research, the probability distribution of the construction dead loads is considered to be comparable to that of occupancy dead loads, proposed by Ellingwood et al. (1980), i.e. normal distribution with a mean-to-nominal value ($\overline{D} / D_n$ or λ_D) of 1.05 and a coefficient of variation (V_D) of 0.1.

The construction live loads normally include the weight of labourers, equipment, and stacked materials. The probabilistic data on construction live loads is limited and dependent on the stage of construction; moreover, the fitted distribution can be complex. Karshenas and Ayoub (1994b) reported statistical data of the surveyed live loads conducted before concrete placement in the period of 1987 to 1990 on over twenty two concrete building sites in the Unites States. They recommended a mixed probability distribution consisting of a discrete part at zero loads and a continuous exponential distribution at nonzero loads. The same researchers (Karshenas and Ayoub 1994a) also studied construction live loads on slab formworks after concrete placement. The mean of the construction live loads on newly poured slabs, (surveyed 1 week after the pour), was calculated to be 0.3 kPa with a very high coefficient of variation of 1.10. The result was later used in the research by Rosowsky and Stewart (2001) to simulate the distribution of maximum construction live loads over the period of 6 months using a Monte Carlo method. A type I extreme value distribution was found to give the best fit to the simulated distributions of measured construction live loads. Also, Rosowsky (1996) reported on the development of the new ASCE standard on load combinations and load factors for construction. Rosowsky implied that since there was little data available on probabilistic models for construction loads, the code had been developed based on conservative judgment and consensus among engineers. Ellingwood and Galambos (1982) reported that statistical data on live loads for buildings and conventional structures may be modelled as a type I extreme value distribution with $\overline{L} / L_n = 1.0$ and a coefficient of variation (V_L) of 0.25. In this research, the probability distribution of the construction live loads is assumed to be type I extreme value distribution with a mean-to-nominal value ($\overline{L} / L_n$ or λ_L) of 1.0 and a conservative coefficient of variation (V_L) of 0.6. Table 10 summarises the construction load statistics used in this research.

Table 10: Statistics for construction loads

Load	Mean-to-nominal value	Coefficient of variation	Probability distribution
Dead	1.05	0.1	Normal
Live	1.0	0.6	Type I extreme value

5.2 SYSTEM RESISTANCE FACTORS

Based on the LRFD design formulae of $\varphi_{system}R_n = 1.2D_n + 1.6L_n$ (ASCE 2005) and $\varphi_{system}R_n = 1.25D_n + 1.5L_n$ (Standard Australia 1995), the system resistance factors φ_{system} can be computed for various system configurations using the code calibration procedure discussed in Section 5. The nominal live-to-dead load ratio (L_n/D_n) is assumed to be 0.5. Typical L_n/D_n ratios for reinforced concrete structures are in the range of 0.5-1.5 (Ellingwood et al. 1980), and the design of support scaffold systems is usually critical in the stage of concrete pouring as suggested by Hadipriono and Wang (1987). An L_n/D_n ratio of 0.5 is a reasonably representative value since the construction live loads such as the weight of labourers, small equipment, and mounding of concrete are relatively small compared to the dead loads from the weight of wet concrete, steel reinforcement, and formwork. Other probabilistic parameters for the code calibration have been presented earlier in Sections 4.3 and 5.1. Because the L_n/D_n ratio is assumed to be 0.5, both LRFD design formulae herein give identical results of system resistance factor through a reliability analysis, which can be verified by Eq. (4) and exemplified in Figure 46. Since the mean-to-nominal ratios and coefficients of variation of the system resistances of different system sizes (1x1, 3x3, 3x6, and 9x9 bays) with the same lift height and jack extensions (see Table 9) are comparable, then the system resistance factors can be categorised based on the lift height and top and bottom jack extensions. The results of the system resistance factor for a system reliability index in the range of 3.0-5.0, as obtained from an FORM reliability analysis for different system configurations, are presented in Figures 47-49.

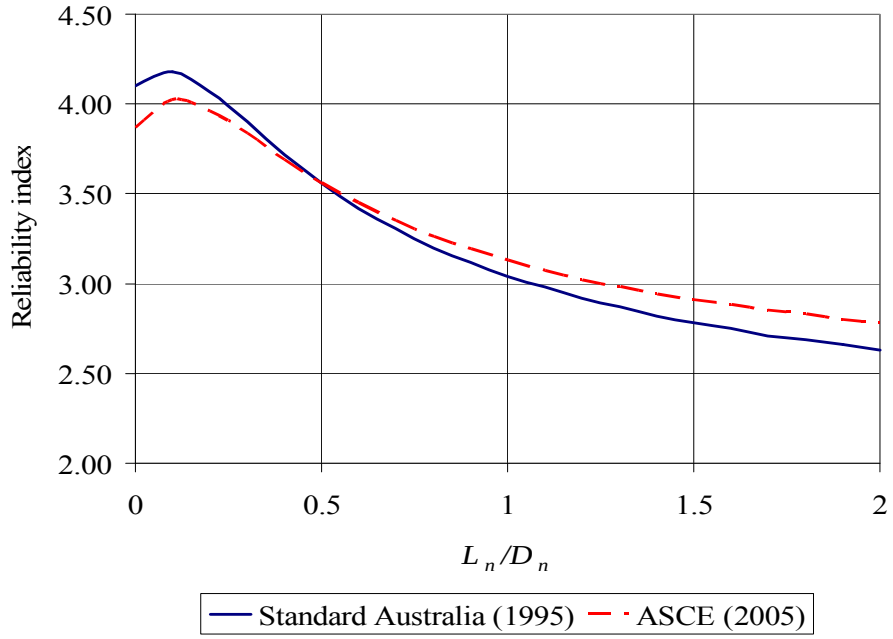

Figure 46: Comparison between Australian and ASCE design formulae based on L_n/D_n

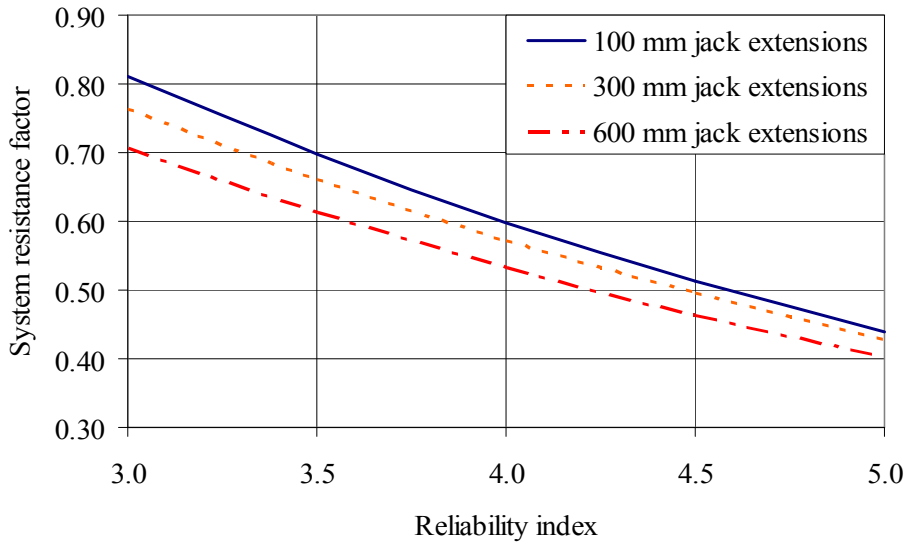

Figure 47: System resistance factor for 1.0 m lift scaffold system

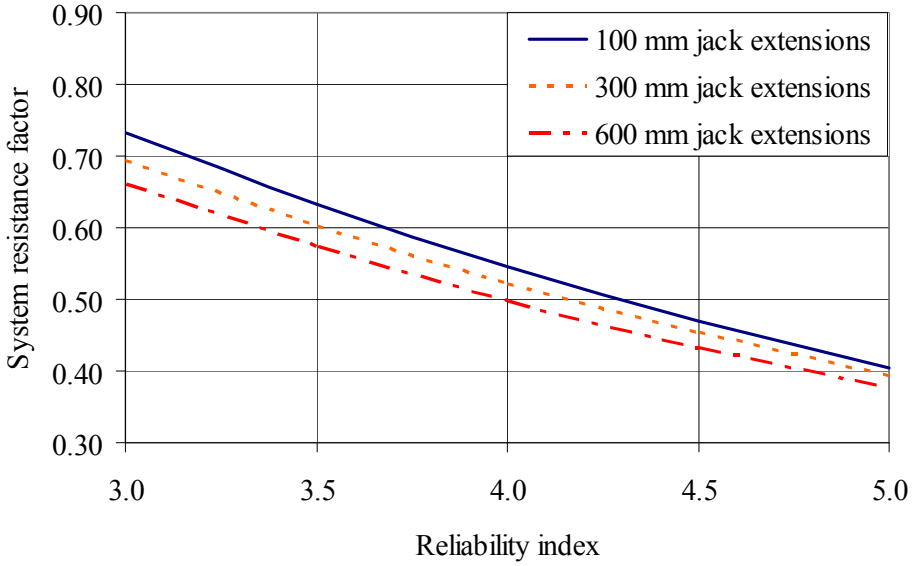

Figure 48: System resistance factor for 1.5 m lift scaffold system

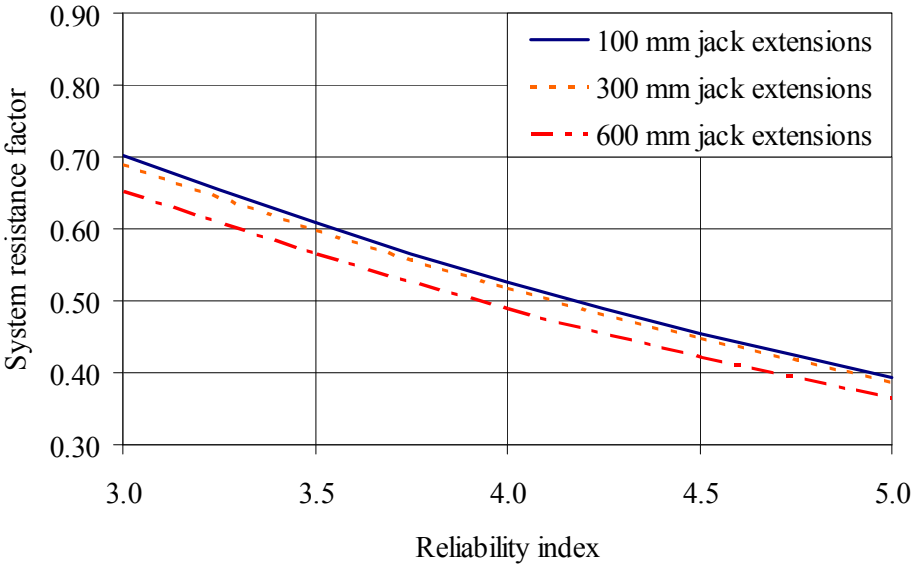

Figure 49: System resistance factor for 2.0 m lift scaffold system

It appears from the figures that the system resistance factor φ_{system} can be as low as 0.37 if the system target reliability index is chosen as 5.0, and as high as 0.81 if the system target reliability index is chosen as 3.0. In addition, longer jack extensions and higher lift heights have lower system resistance factors for the same system target reliability index. In terms of system reliability index, some researchers have recommended values in the range of 2.5 to 4 depending on the risk of failure and type of structures (Galambos 1990). In this research, the system target reliability of 3.5 is deemed appropriate as recommended by Galambos (1990) for a frame suffering complete damage (no expected loss of life) when buckling under the action of gravity loads with little assistance from claddings. Table 11 presents the system resistance factors φ_{system}, determined for the system target reliability index of 3.5 for support scaffold systems and categorised by the lift height and top and bottom jack extensions. The mean-to-nominal ratio for system resistance ($\overline{R} / R_n$) and corresponding coefficient of variation (V_R) for each system configuration are also shown. The load statistics are as described in Section 5.1. The values of system resistance factor are presented for both FOSM and FORM calibration procedures; however, the system resistance factor φ_{system} determined by the FORM is recommended in view of enhanced accuracy.

Table 11: System resistance factors for support scaffold systems (β = 3.5)

Lift height (m)	Jack extensions (mm)	$\overline{R} / R_n$	V_R	φ_{system} (FOSM)	φ_{system} (FORM)
1.0	100	1.35	0.13	0.78	0.70
1.0	300	1.23	0.11	0.77	0.66
1.0	600	1.12	0.10	0.72	0.61
1.5	100	1.20	0.12	0.72	0.63
1.5	300	1.10	0.10	0.71	0.60
1.5	600	1.05	0.10	0.68	0.57
2.0	100	1.13	0.11	0.70	0.61
2.0	300	1.11	0.11	0.69	0.60
2.0	600	1.05	0.11	0.65	0.56

In all cases, the system resistance factors based on FORM are shown to be smaller than those based on FOSM because the probability distributions assumed herein are more conservative than those (normal distributions) of the FOSM. To calculate the system resistance factor for other jack extensions, linear

interpolation can be applied, i.e. φ_{system} = 0.66 + (400 – 300) (0.61 – 0.66) / (600 – 300) = 0.64 for 1.0 m lift height with 400 mm jack extensions. In the design of support scaffold systems, it might not be possible to specify the same jack extension for all standards since the ground or formwork might not be level. In such situations, the system resistance factor φ_{system} can be based on only the lift height by averaging the values for different jack extensions such that for 1.0 m lift, φ_{system} = 0.66, for 1.5 m lift, φ_{system} = 0.60, and for 2.0 m lift, φ_{system} = 0.59.

6 CONCLUSIONS

This research report presents comprehensive studies of the effects of uncertainties in material properties, initial geometric imperfections, and joint stiffness on the ultimate strength of steel support scaffold systems through a rational statistical framework and a second-order inelastic finite element (advanced) analysis. The report also presents a reliability analysis of support scaffold systems to determine system resistance factors that can be used in the direct design by advanced analysis according to the LRFD framework. Having procured the statistical data for the main random variables affecting the strength of support scaffold systems in previous studies (Chandrangsu and Rasmussen 2008; Chandrangsu and Rasmussen 2009a), Monte Carlo simulations are carried out to determine the statistical distributions of strength for a range of configurations of support scaffold systems. The load statistics are considered for the gravity load combination. The first-order second-moment method (FOSM) and first-order reliability method (FORM) are then employed for determining the system resistance factors for support scaffold systems in various system configurations. Finally, the system resistance factors, φ_{system}, determined by FORM for a system target reliability index of 3.5 and categorised by the lift height and jack extensions, are proposed to be used in the LRFD design of support scaffold systems by advanced analysis. The proposed system resistance factors vary from 0.56 to 0.70, depending on the lift height and jack extensions.

ACKNOWLEDGMENTS

The authors would like to thank Boral Formwork & Scaffolding Pty Ltd and the Australian Research Council for providing financial and in-kind support for this research project through Linkage Grant LP0884156 “High-strength formwork systems”.

REFERENCES

ASCE. (2005). "Minimum design loads for buildings and other structures. ASCE 7-05." American Society of Civil Engineers, New York.

Ayyub, B. M., and McCuen, R. H. (2003). *Probability, statistics, and reliability for engineers and scientists*, Chapman Hall/CRC, Boca Raton, Florida.

Bulleit, W. M. (2008). "Uncertainty in structural engineering." *Practice Periodical on Structural Design and Construction*, 13(1), 24-30.

Buonopane, S. G., and Schafer, B. W. (2006). "Reliability of steel frames designed with advanced analysis." *Journal of Structural Engineering*, 132(2), 267-276.

CASE. (2006). "Tests of formwork subassemblies and components. Investigation Report No. S1499." Centre for Advanced Structural Engineering, School of Civil Engineering, University of Sydney.

Chandrangsu, T., and Rasmussen, K. J. R. (2008). "Scaffold Cuplok joint tests. Research Report No. 893." Centre for Advanced Structural Engineering, School of Civil Engineering, University of Sydney.

Chandrangsu, T., and Rasmussen, K. J. R. (2009a). "Investigation of geometric imperfections of support scaffold systems. Research Report No. 895." Centre for Advanced Structural Engineering, School of Civil Engineering, University of Sydney.

Chandrangsu, T., and Rasmussen, K. J. R. (2009b). "Structural modelling of support scaffold systems. Research Report No. 896." Centre for Advanced Structural Engineering, School of Civil Engineering, University of Sydney.

Ellingwood, B., and Galambos, T. V. (1982). "Probability-based criteria for structural design." *Structural Safety*, 1, 15-26.

Ellingwood, B., Galambos, T. V., MacGregor, J. G., and Cornell, C. A. (1980). "Development of a probability-based load criterion for American National Standard A58, NBS special publication 577." National Bureau of Standards, Washington, D.C.

Galambos, T. V. (1990). "Systems reliability and structural design." *Structural Safety*, 7(2-4), 101-108.

Galambos, T. V., and Ravindra, M. K. (1978). "Properties of steel for use in LRFD." *Journal of the Structural Division, American Society of Civil Engineers*, 104(9), 1459-1468.

Hadipriono, F. C., and Wang, H. K. (1987). "Causes of falsework collapses during construction." *Structural Safety*, 4(3), 179-195.

Karshenas, S., and Ayoub, H. (1994a). "Analysis of concrete construction live loads on newly poured slabs." *Journal of Structural Engineering*, 120(5), 1525-1542.

Karshenas, S., and Ayoub, H. (1994b). "Construction live loads on slab formworks before concrete placement." *Structural Safety*, 14(3), 155-172.

Melchers, R. E. (1999). *Structural reliability analysis and prediction*, John Wiley & Sons Ltd, West Sussex, England.

Nowak, A. S., and Collins, K. R. (2000). *Reliability of structures*, McGraw-Hill, New York.

Rosowsky, D. V. (1996). "Load combinations and load factors for construction." *Journal of Performance of Constructed Facilities*, 10(4), 175-181.

Rosowsky, D. V., and Stewart, M. G. (2001). "Probabilistic construction load model for multistory reinforced-concrete buildings." *Journal of Performance of Constructed Facilities*, 15(4), 145-152.

Standard Australia. (1995). "AS 3610: Formwork for concrete."

Standard Australia. (1998). "AS 4100: Steel structures."

Strand7. (2009). "Strand7 release 2.4.1 manual." Strand7 Pty Ltd.